

AD-A150 533

CURRENT PROBLEMS IN TURBOMACHINERY FLUID DYNAMICS(U)  
MASSACHUSETTS INST OF TECH CAMBRIDGE GAS TURBINE LAB  
E M GREITZER ET AL. 03 DEC 84 AFOSR-TR-85-0016

1/1

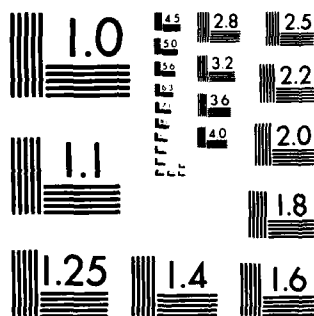
UNCLASSIFIED

F49620-82-K-0002

F/G 21/5

NL

END



MICROCOPY RESOLUTION TEST CHART  
NATIONAL BUREAU OF STANDARDS-1963-A

UNCLASSIFIED

SECURITY CLASSIFICATION OF THIS PAGE

AD-A150 533

13

1a. REPORT SECURITY CLASSIFICATION Unclassified		1b. RESTRICTIVE MARKINGS None	
2a. SECURITY CLASSIFICATION AUTHORITY		3. DISTRIBUTION/AVAILABILITY OF REPORT Approved for public release; distribution unlimited.	
2b. DECLASSIFICATION/DOWNGRADING SCHEDULE			
4. PERFORMING ORGANIZATION REPORT NUMBER(S)		5. MONITORING ORGANIZATION REPORT NUMBER(S) <b>AFOSR-TR- 85 - 0016</b>	
6a. NAME OF PERFORMING ORGANIZATION Department of Aeronautics and Astronautics	6b. OFFICE SYMBOL (If applicable) 31-264	7a. NAME OF MONITORING ORGANIZATION See #8	
6c. ADDRESS (City, State and ZIP Code) <b>MIT</b> Cambridge, MA 02139		7b. ADDRESS (City, State and ZIP Code) See #8 <b>SELECTED</b> <b>FEB 21 1985</b>	
8a. NAME OF FUNDING/SPONSORING ORGANIZATION Air Force Office of Scientific	8b. OFFICE SYMBOL (If applicable) Research	9. PROCUREMENT INSTRUMENT IDENTIFICATION NUMBER Contract No. F49620-82-K-0002	
8c. ADDRESS (City, State and ZIP Code) AFOSR Bolling AFB, DC 20332		10. SOURCE OF FUNDING NOS.	
		PROGRAM ELEMENT NO. <b>61102F</b>	TASK NO. <b>A4</b>
11. TITLE (Include Security Classification) Current Problems in Turbomachinery Fluid Dynamics		<b>(UNCLASSIFIED)</b>	
12. PERSONAL AUTHOR(S) E.M. Greitzer, J.L. Kerrebrock, W.T. Thompkins, J.E. McCune, A.H. Epstein, W.R. Hawthorne, C. S.			
13a. TYPE OF REPORT Final Report	13b. TIME COVERED FROM <b>10/1/81</b> TO <b>9/30/84</b>	14. DATE OF REPORT (Yr., Mo., Day) <b>12/3/84</b>	15. PAGE COUNT 54
16. SUPPLEMENTARY NOTATION			
17. COSATI CODES		18. SUBJECT TERMS (Continue on reverse if necessary and identify by block number)	
FIELD	GROUP	SUB. GR.	
		Transonic Compressors, Compressor Stability, Casing Treatment, Inlet Vortex, Turbomachinery Design, Heavily Loaded Compressors	
19. ABSTRACT (Continue on reverse if necessary and identify by block number)			
A multi-investigator program on problems of current interest in turbomachinery fluid dynamics is being conducted at the MIT Gas Turbine Laboratory. Within the scope of this effort, four different tasks, encompassing both design and off-design problems, have been identified. These are: (1) Investigation of fan and compressor design point fluid dynamics (including formation of design procedures using current 3-D transonic codes and development of advanced measurement techniques for use in transonic fans); (2) Studies of basic mechanisms of compressor stability enhancement using compressor casing/hub treatment; (3) Fluid mechanics of inlet vortex flow distortions in gas turbine engines; and (4) Investigations of 3-D analytical and numerical computations of flows in highly loaded turbomachinery blading. In addition to these tasks, this multi-investigator effort also includes the Air Force Research in Aero Propulsion Technology (AFRAPT) Program. This document describes work carried out on this contract during the period 10/1/81 - 9/30/84.			
20. DISTRIBUTION/AVAILABILITY OF ABSTRACT UNCLASSIFIED/UNLIMITED <input checked="" type="checkbox"/> SAME AS RPT. <input type="checkbox"/> DTIC USERS <input type="checkbox"/>		21. ABSTRACT SECURITY CLASSIFICATION <b>UNCLASSIFIED</b>	
22a. NAME OF RESPONSIBLE INDIVIDUAL <b>Dr James D. Wilson</b>		22b. TELEPHONE NUMBER (Include Area Code) <b>202/767-4135</b>	22c. OFFICE SYMBOL <b>AFOSR/NA</b>

DD FORM 1473, 83 APR

EDITION OF 1 JAN 73 IS OBSOLETE.

85

127

UNCLASSIFIED  
SECURITY CLASSIFICATION OF THIS PAGE

DNC FILE COPY

AFOSR-TR. 85-0016

GAS TURBINE LABORATORY  
DEPARTMENT OF AERONAUTICS AND ASTRONAUTICS  
MASSACHUSETTS INSTITUTE OF TECHNOLOGY  
CAMBRIDGE, MA 02139

FINAL REPORT

on

CONTRACT NO. F49620-82-K-0002

entitled

CURRENT PROBLEMS IN TURBOMACHINERY FLUID DYNAMICS

for the period

October 1, 1981 to September 30, 1984

submitted to

AIR FORCE OFFICE OF SCIENTIFIC RESEARCH

Attention: Dr. James D. Wilson, Program Manager  
Directorate of Aerospace Sciences, AFOSR (AFSC)  
Bolling Air Force Base, DC 20332

Principal  
Investigators: Edward M. Greitzer  
Jack L. Kerrebrock  
William T. Thompkins, Jr.  
James E. McCune

Co-Investigators: Alan H. Epstein  
Choon S. Tan

Collaborating  
Investigators: Eugene E. Covert  
Sir William R. Hawthorne  
Wai K. Cheng  
Hyouun-Woo Shin  
Robert Haines

November 1984



Approved for public release;  
distribution unlimited.

F49620-82-K-0002

## TABLE OF CONTENTS

<u>SECTION</u>	<u>PAGE</u>
1. INTRODUCTION	1
2. RESEARCH TASKS	3
Task I:    Investigation of Fan and Compressor Design Point Fluid Dynamics	3
A.    Inverse Design Task	3
B.    Loss Mechanisms and Loss Migration in Transonic Compressors	8
Task II:   Mechanisms of Stability Enhancement Using Casing/Hub Treatment	11
Task III:  Inlet Vortex Flow Distortions in Gas Turbine Engines	18
Task IV:   Investigation of Discrete-Blade and Three- Dimensional Flows in Highly Loaded Turbomachines	23
A.    3D Blade Design in Highly-Loaded Axial Compressors	23
B.    Numerical Study of Secondary Flow in a Bend Using Spectral Methods	30
C.    Non-Axisymmetric Compressible Swirling Flow in Turbomachine Annuli	47
3. PROGRAM PERSONNEL	48
4. INTERACTIONS	50
5. DISCOVERIES, INVENTIONS AND SCIENTIFIC APPLICATIONS	51
6. SUMMARY AND CONCLUSIONS	52

AIR FORCE OFFICE OF SCIENTIFIC RESEARCH (AFSC)  
NOTICE OF TRANSMITTAL TO DTIC  
This technical report has been reviewed and is  
approved for public release (AFR 19-12).  
Distribution is unlimited.  
MATTHEW J. KESPER  
Chief, Technical Information Division

## 1. INTRODUCTION

This is a final report on work carried out at the Gas Turbine Laboratory at MIT, as part of our multi-investigator effort on current problems in turbomachinery fluid dynamics. Support for this program was provided by the Air Force Office of Scientific Research under Contract Number F49620-82-K-0002, Major M.S. Francis and Dr. J.D. Wilson, Program Managers.

The present report gives a summary of the work for the period 10/1/81 to 9/30/84. For further details and background, the referenced reports, publications and the previous progress reports [1,2,3,4,5], which go into considerable depth, should be consulted.

Within the general area of turbomachinery fluid dynamics, four separate tasks are specified under this contract. These are, in brief:

1. Investigation of fan and compressor design point fluid dynamics,
2. Studies of compressor stability enhancement,
3. Fluid mechanics of gas turbine operation in inlet flow distortion,
4. Investigations of three-dimensional flows in highly loaded turbomachines.

In addition to these tasks, the multi-investigator contract also encompassed the Air Force Research in Aero Propulsion Technology program. The work carried out in each of the tasks will be described in the next section. Publications generated are listed in these individual task descriptions.

As stated, the present report is intended, with one exception, to be only a description of the highlights of the work carried out during the contract period. The one exception is in the area of spectral method

calculations of three-dimensional viscous flows in turbomachines. These results have only recently been obtained, and there is hence little mention of them in previous reports. For this reason, they are presented in somewhat more detail than the other projects.

#### References

1. E.M. Greitzer, et al., AFOSR TR-82-0027, Final Report, 10/79 - 9/81, on "Current Problems in Turbomachinery Fluid Dynamics."
2. E.M. Greitzer, et al., Annual Report, 10/1/81 - 11/30/82, on "Current Problems in Turbomachinery Fluid Dynamics."
3. E.M. Greitzer, et al., Semi-Annual Report, 12/1/82 - 5/31/83, on "Current Problems in Turbomachinery Fluid Dynamics."
4. E.M. Greitzer, et al., Annual Report, 12/1/82 - 10/31/83, on "Current Problems in Turbomachinery Fluid Dynamics."
5. E.M. Greitzer, et al., Semi-Annual Report, 11/1/83 - 5/31/84, on "Current Problems in Turbomachinery Fluid Dynamics."

## TASK I: INVESTIGATION OF FAN AND COMPRESSOR DESIGN POINT FLUID DYNAMICS

### A. INVERSE DESIGN TASK

During the last three years, efforts on the inverse design project have been directed to finding an inverse or design method which was applicable to the full Mach number range encountered in high speed axial compressors. We have found one method, based on time marching solutions to the Euler equations, which is accurate enough and could potentially be extended to three-dimensional geometries, see Refs. [1,2,3,4]. This method operates in a mixed mode format in which either blade pressure distributions or geometric constraints are specified. The method is unfortunately far too slow, in terms of computer time usage, for practical design work and, in its present form, does not properly adjust solid wall positions in subsonic flow regions.

Work on the time-marching-like method is now considered complete with the publication of a PhD thesis on the method by Tong [4]. This thesis contains new information about sources of numerical errors in finite difference solutions and artificial smoothing operators, a demonstration that the simple inverse scheme would work in supersonic flow but not in mixed subsonic-supersonic flows, and a survey and evaluation of existing inverse and design methods.

A new inverse method has been developed which is many times faster than the old time marching scheme, is easily coupled to boundary layer solvers and is more accurate than the time marching style solvers, see Ref. [5]. This new method appears to retain all the traditional advantages of streamline curvature schemes while being useful for subsonic, supersonic,



transonic, and shocked flows. The scheme can be described as a conservative finite volume scheme in streamline coordinates and has been applied to supersonic duct flows, subsonic and transonic duct flows, subsonic cascade flows, and viscous-inviscid interactions.

Some of the most interesting results from this work are shown in Figs. 1 through 3. Figure 1 shows an inverse mode calculation for a supersonic jet flow. The periodic shock diamond structure characteristic of these flows is clearly visible. Figure 2 shows calculated streamlines and Mach number contours for an axial turbine cascade. This calculation was done both in the direct mode and the inverse mode to demonstrate the applicability of the scheme to flows in cascades. Figure 3 shows the results from a test of the viscous-inviscid coupling procedure for a subsonic duct flow with separation. This test demonstrated that the streamtube method could be coupled with a boundary layer solver to include some viscous effects, but the coupling algorithm is presently unstable for transonic flows. Further work is continuing in this area.

#### References

1. Thompkins, W.T. and Tong, S.S., "Inverse or Design Calculations for Non-Potential Flow in Turbomachinery Blade Passages," Trans. of ASME, J. Eng. Power, Vol. 104, No. 2, April 1982.
2. Tong, S.S. and Thompkins, W.T., "A Design Calculation Procedure for Shock-Free or Strong Passage Shock Turbomachinery Cascades," Trans. of ASME, J. Eng. Power, Vol. 105, No. 2, April 1983.
3. Thompkins, W.T., Tong, S.S., Bush, R.H., Usab, W.J.Jr., Norton, R.J.G., "Solution Procedures for Accurate Numerical Simulations of Flow in Turbomachinery Cascades," AIAA Paper 83-257, presented at AIAA 21st Aerospace Sciences Meeting, Jan. 9-13, 1983, Reno, Nevada.
4. Tong, S.S., "Procedures for Accurate Inviscid Flow Simulations and Profile Refinement of Turbomachinery Cascades," PhD Thesis, MIT, February 1984.
5. Drela, M., Giles, M., and Thompkins, W.T., "Conservative Streamtube Solution of Steady State Euler Equations," AIAA Paper 84-1643, June 1984.

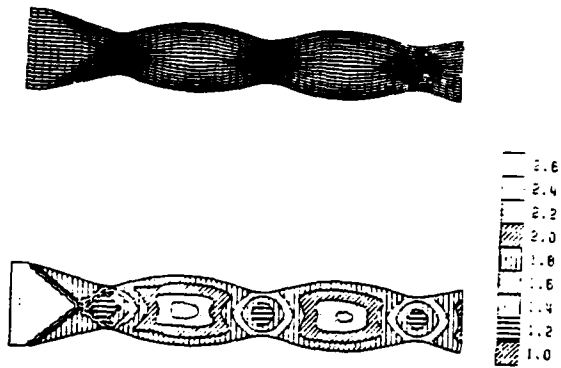


Figure 1 - Streamlines and Mach number contours  
for supersonic jet

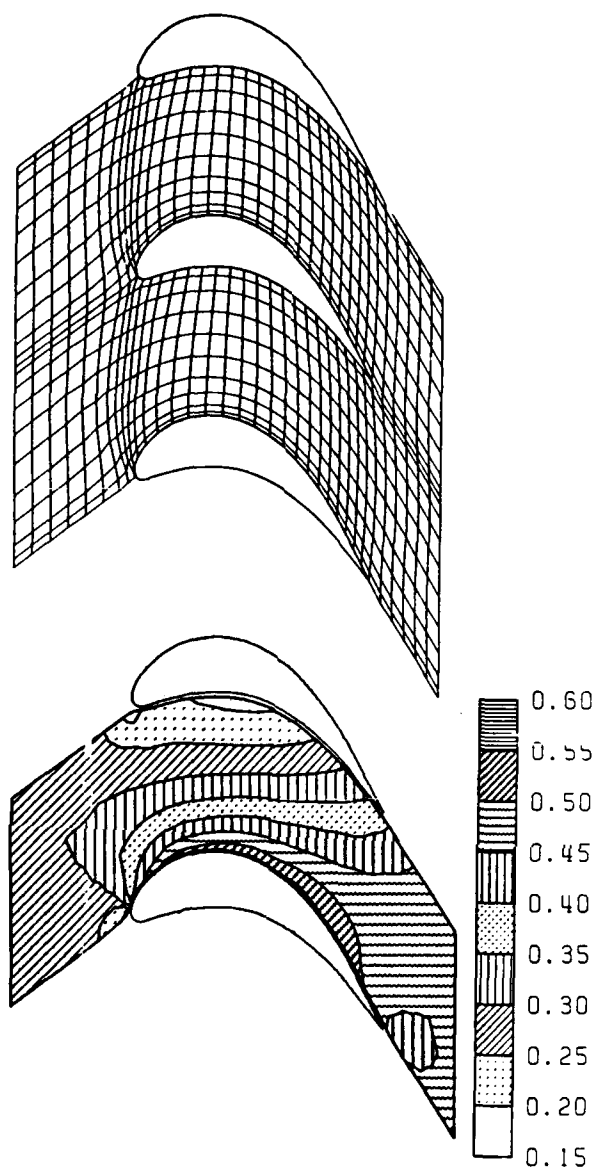


Figure 2 - Streamlines and Mach number contours  
for turbine cascade

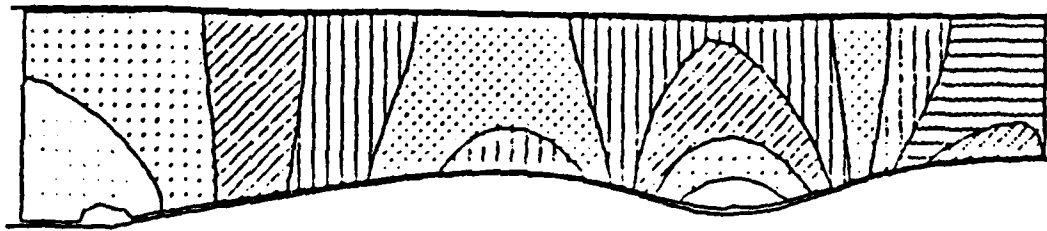
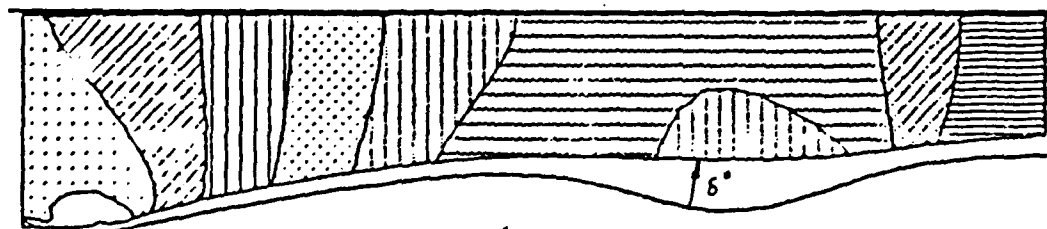


FIGURE 3A - Mach number contour plot without boundary layer interaction



$Re = 10^4$

FIGURE 3B - Mach number contour-plot with boundary layer interaction

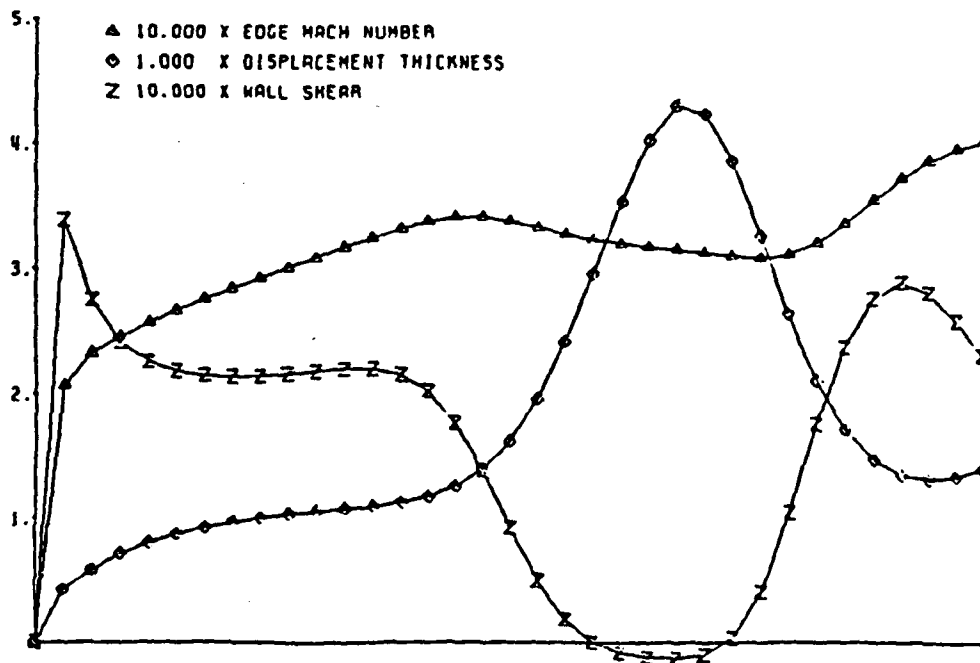


FIGURE 3C - Boundary layer parameters for interaction calculation

Viscous-Inviscid Interaction Calculation for Duct Flow

## IB. LOSS MECHANISMS AND LOSS MIGRATION IN TRANSONIC COMPRESSORS

Under the sponsorship of AFOSR, MIT has been studying the time-resolved flowfield in transonic compressor stages in order to elucidate the physical mechanisms responsible for compressor loss. This study was facilitated by the invention of an instrument capable of instantaneous measurement of gas total temperature and pressure, thus permitting the first detailed spatial and temporal map of stage efficiency [1,2,3].

The instrument is an aspirating probe, which consists of a pair of constant temperature hot wires in a 1.5 mm diameter channel with a choked exit. In the constant Mach number flow in the channel, the heat loss from the wires is influenced only by freestream total temperature and pressure. By operating the wires at different temperatures in separate constant temperature anemometer circuits, two simultaneous voltage measurements are made from which the two unknowns, stagnation temperature and pressure, can be determined. The present design has good response from dc to 20 kHz.

The aspirating probe was used to measure the flowfield in a high throughflow transonic compressor stage in the MIT Blowdown Compressor Facility. Data were also obtained by surveys with a high response angle probe and with tip-casing transducers. Test results showed that the stagnation temperature, calculated with the Euler equation using measured tangential flow Mach number from the angle probe, agreed well with direct measurement of stagnation temperature from the aspirating probe. The time-resolved data also exhibited pressure and temperature fluctuations in the inviscid core flow at a frequency of 3 to 5 times blade passing with an

amplitude of  $1/2$  of the wake total pressure defect. A basic fluid dynamic model was presented which explains these fluctuations as a result of unsteadiness in the blade shockwave positions. Considering the complexity of the flow and the inherent simplifying assumptions, the comparisons between experiment and theory are reasonable.

Simple mixing calculations show that, as an upper bound, the high frequency unsteadiness contributes on the order of 1% of the rotor loss. Conventional steady-state instrumentation may give misleading results in this flow since the loss associated with the fluctuations does not appear directly at the rotor exit.

The data obtained from wall static measurements and probes held at a fixed immersion at rotor exit show a low frequency oscillation (67 Hz). The disturbance occurs throughout the entire span of the rotor and disappears in less than half a rotor chord, both upstream and downstream. Although the origin of this low frequency disturbance is not well understood yet, the observed phenomenon is believed to be inherent to transonic rotors, and may have significant impact on data interpretation for steady state test rigs, and the aerodynamic performance of transonic compressor stages.

The development of the aspirating probe offers the opportunity, for the first time, of accurate gas injection flow tracing in a transonic compressor, since the probe is capable of differentiating between simultaneous variations in temperature, pressure, and species concentration. Hence, during the past several months, we have been investigating the use of the aspirating probe as a way of examining the unsteady radial flow transport of the fluid in rotor passages using a gas injection technique.

The aim is to clarify the importance of radial transport in the fluid physics of transonic compressors, and the effect of such transport on efficiency in particular. The principle research vehicle will be the AFAPL High Thru Stage in the MIT Blowdown Compressor Tunnel.

#### References

1. Ng, W.F., "Time-Resolved Stagnation Temperature Measurement in a Transonic Compressor Stage," MIT GTL Report No. 177, October 1983.
2. Ng, W.F. and Epstein, A.H., "High Frequency Temperature and Pressure Probe for Unsteady Compressible Flows," American Institute of Physics Review of Scientific Instruments, December 1983.
3. Ng, W.F. and Epstein, A.H., "Unsteady Losses in Transonic Compressors," ASME paper 84-GT-183, presented at 29th International Gas Turbine Conference and Exhibit, Amsterdam, The Netherlands, June 4-7, 1984.

## TASK II: MECHANISMS OF STABILITY ENHANCEMENT USING CASING/HUB TREATMENT

This project is aimed at understanding the basic mechanisms by which a grooved casing over the tip of a compressor rotor is able to substantially increase the stable operating range of the machine. Such configurations have been used for over a decade, in both axial and centrifugal compressors. Although they have been incorporated into actual aircraft engines, there is still no fundamental understanding of how they work, and their application is still very much on a "cut and try" basis.

Several tasks have been accomplished on this project. First, since it was clear from the outset that some detailed experimental investigations would be needed, the initial work involved refurbishing (and modernizing) the MIT Low Speed Single Stage Compressor.

Early in the project, it was decided that a very useful approach would be the use of a grooved hub which rotated under a cantilevered stator row. It was hypothesized that, although there had been several unsuccessful attempts with this type of configuration, a properly designed "hub treatment" should be able to provide a large increase in stable flow range. If so, it would not only provide a simpler situation from which to investigate the flow in the endwall region of the blade passage, but might give a different perspective from which to view the phenomenon.

A basic task associated with the use of this type of treatment was to ensure that there was a "wall stall" at the hub. The absence of this situation was felt to be the reason why previous hub treatments had not worked. The general plan was to set up a wall stall situation with both a



smooth hub and a grooved hub and examine in detail the differences.

In addition to this, however, it was also desired to investigate the basic premise of wall stall, rather than blade stall, as a requisite for casing/hub treatment to be effective [1,2]. Thus, two different geometries were defined, one for wall stall at the hub and one for blade stall. The choice of configuration is described in [1], but basically the central differences between the two were higher stagger and larger tip clearance for the wall stall configuration.

A further requirement for the application of hub treatment, of course, is that the stator hub be the element that stalls. Thus, inherent in the design of the two configurations was the restaggering of the rotor so that it was matched far away from stall and served merely as a flow generator. New inlet guide vanes were also designed as part of this. Finally, the stator was deliberately spaced away from the rotor in order to decouple it from the rotor and inlet guide vanes. These two rows thus served only as a "flow generator" to provide a swirling flow to the stator. The grooves used in the hub were axial skewed grooves, which were known to give a large increase in stall margin when used as casing treatment. A schematic of the compressor is shown in Fig. 1 [1,2].

The experiment was very successful in that both overall aspects were confirmed. First, the hub treatment did indeed increase the stable flow range and peak pressure rise of the stator. Figure 2 shows the stator pressure rise characteristic for the wall stall situation [3]. To the author's knowledge, this is the first time that results of this type have been reported. It can be seen that an increase in peak pressure rise of

over fifty percent was achieved using the grooved treatment. Second, the tests with the blade stall configuration, using the same grooved hub, showed very little improvement, thus giving further confirmation to the basic hypothesis about wall stall versus blade stall.

The more detailed measurements also showed quite interesting results.

As seen in Fig. 3, the stagnation pressure actually increased across the hub section of the stator row for the hub treatment. This implies that significant work is being done by the moving hub on the flow in this region. In addition, there appears to be evidence of a strong jet coming out of the leading edge of these grooves and being deflected downstream by the blades [3]. Whatever the precise configuration of the flow field in the grooves, we think that the flow in and out, which provides a means for bulk momentum interchange, is a crucial element of this phenomenon.

In view of this, the most recent efforts on this project have been aimed at obtaining detailed unsteady measurements inside the blade passages, in the endwall region. During the past year, we have been developing the software and hardware necessary for this. These measurements will be carried out as the first phase of this year's work.

In connection with the question of the momentum interchange, we have also carried out basic control volume analyses of the flow in the endwall region. Although these can only be taken as qualitative, they do indicate that the bulk momentum flux is far more important than turbulent stresses, and that this momentum interchange can drastically affect the stator exit boundary layer. In this regard, the next part of this investigation will involve, as stated, detailed measurements of the unsteady flow and more

quantitative calculations of the interaction of the flow in the grooves with that in the passage endwall.

Finally, it should be mentioned that the present student on this project, M. Johnson, is part of the AFRAPT program.

### Summary and Conclusions

The objectives accomplished under this project were:

1. Upgrading of the MIT Low Speed Compressor.
2. Design of wall stall and blade stall stator rows (rotor IGV serving just as a flow generator).
3. Design of casing and hub treatments.
4. Experimental confirmation, for the first time, of the effectiveness of hub treatment in a wall stall situation - little change when blade stall occurs.
5. Detailed exit measurements which reveal decreased blockage, substantial momentum (and work) interchange between grooved hub and flow in endwall, and strong jet from leading edge of grooves.
6. Calculations which show (qualitatively) that bulk momentum interchange can have a large effect on stator exit flow conditions.
7. Design of hardware and software for detailed unsteady in-passage measurements.

### References

1. Prell, M.E., "An Experimental Investigation of Stator Hub Treatment in an Axial Flow Compressor," MIT GTL Report No. 161, 1981.
2. Greitzer, E.M., "The Stability of Pumping System - The 1980 Freeman Scholar Lecture," J. of Fluids Engineering, Vol. 103, June 1981, pp. 193-242.
3. Cheng, P., Prell, M.E., Greitzer, E.M., Tan, C.S., "Effects of Compressor Hub Treatment on Stator Stall and Pressure Rise," J. Aircraft, Vol. 21, pp. 469-476.

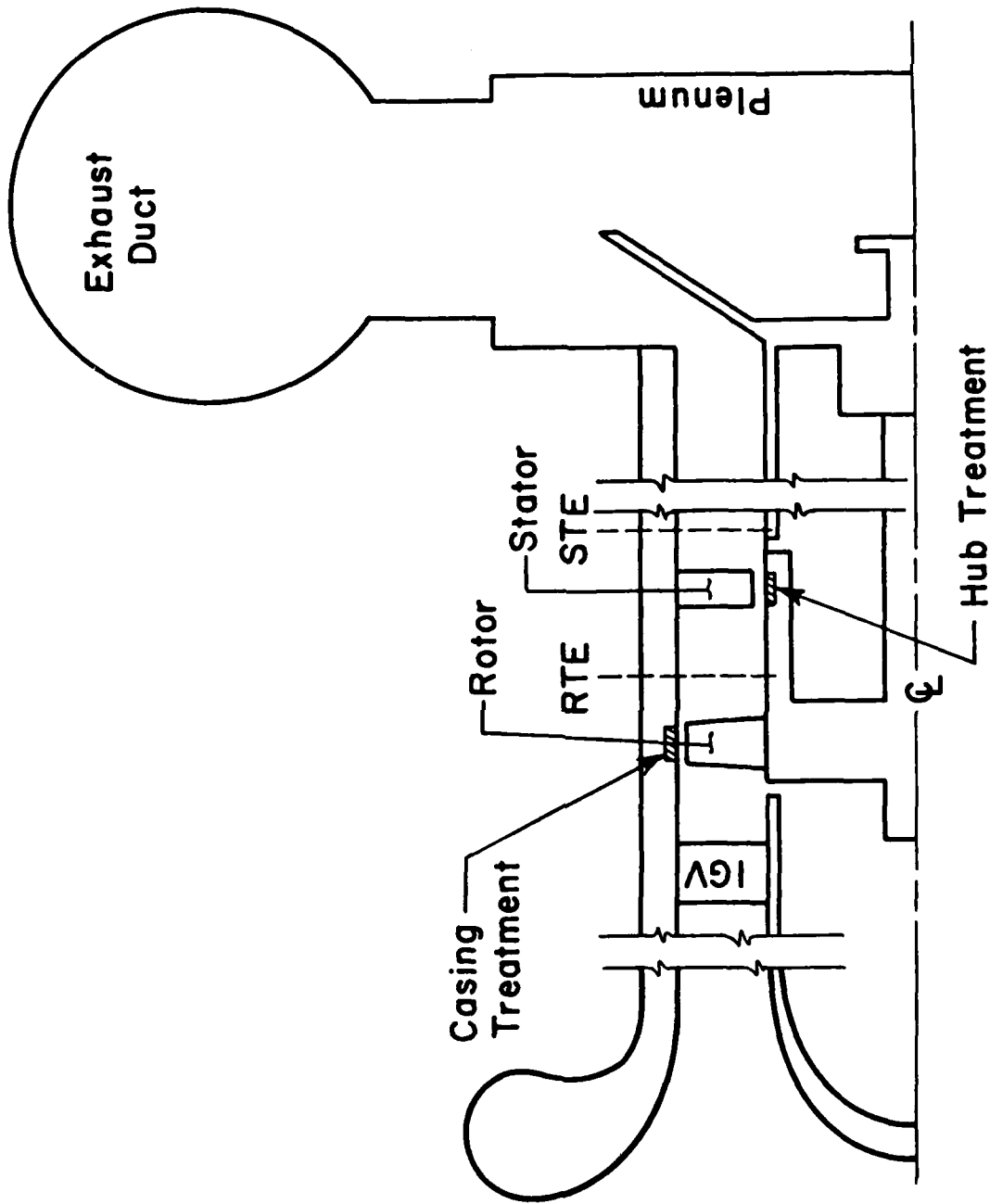


Figure 1: Schematic of Compressor Cross-Section

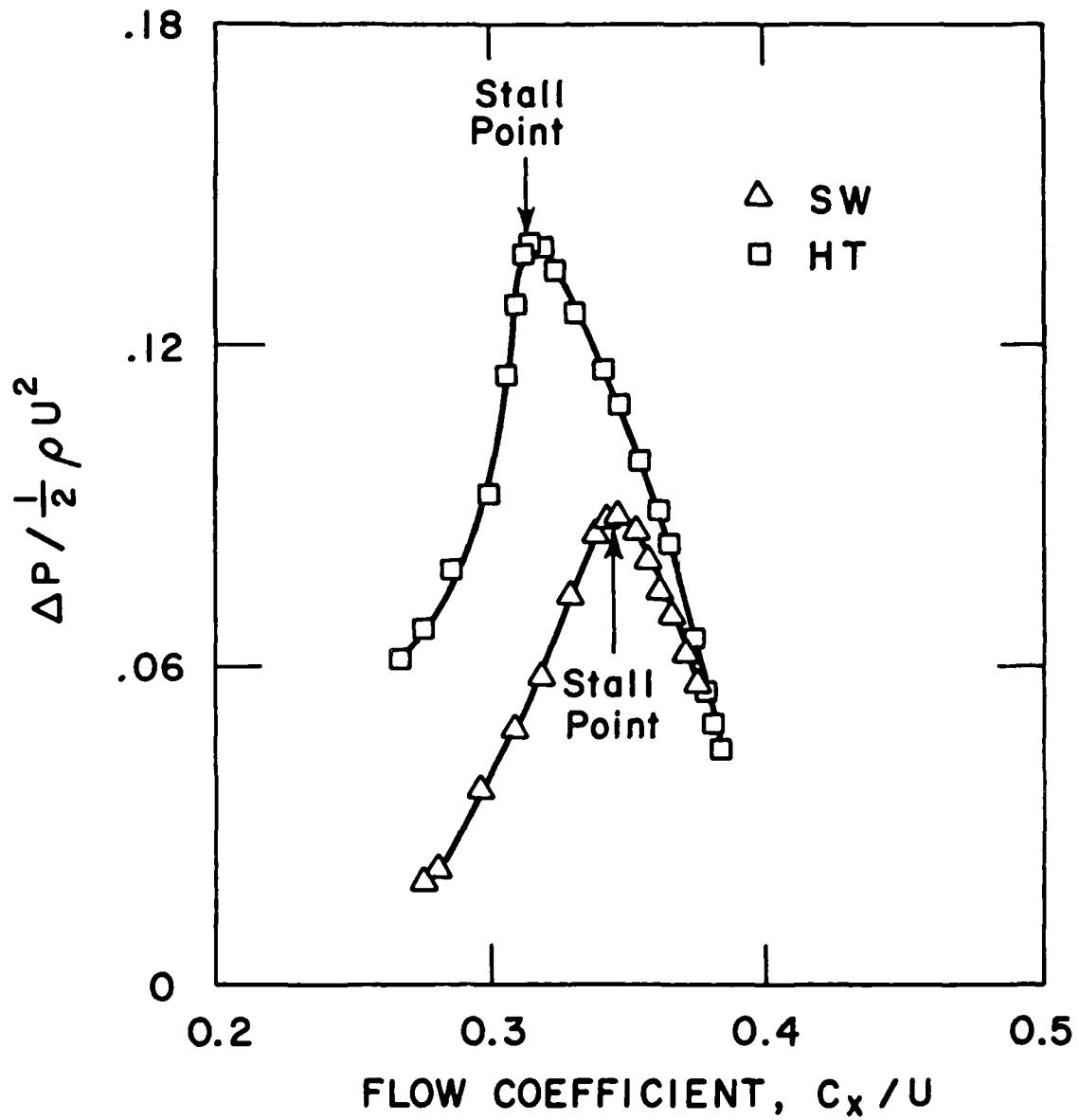


Figure 2: Stator static pressure rise characteristic (high stagger stators) with solid wall (SW) and hub treatment (HT)

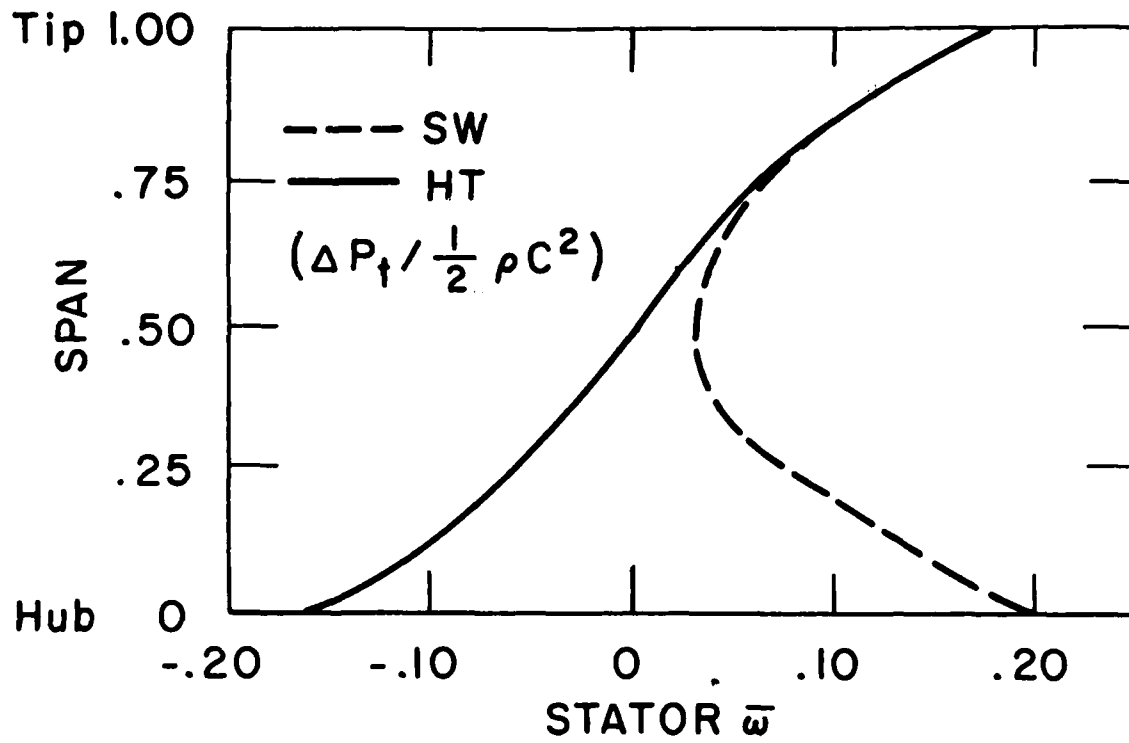


Figure 3: Total pressure change across stator row;  $\bar{\omega} = \Delta P_t / \frac{1}{2} \rho C^2$

## TASK III: INLET VORTEX FLOW DISTORTIONS IN GAS TURBINE ENGINES

This project is focussed on the general area of vortex formation in inlets. Although the original context is that of gas turbine engines, the work is generic in that the same sort of phenomena occur whenever an inlet is operated near a ground plane. In this situation, a strong vortex is often observed to form between the ground plane and the inlet. This can cause such problems as engine surge, foreign object damage, and decreased performance due to erosion from dust ingestion.

Our work during the contract period has addressed two questions:

- 1) What is the mechanism of the formation of these inlet vortices?, and
- 2) What is the magnitude of the vortex that is formed under conditions typical of aircraft engines operated at take-off conditions?

In order to answer the first of these, we have carried out both theoretical and experimental studies of the phenomenon. The initial experiments were carried out in a water tunnel using hydrogen bubble flow visualization [1]. The theoretical study was based on a secondary flow approach in which vortex filaments in a (weak) shear flow were viewed as convected (and deformed) by a three-dimensional primary flow, the latter being calculated numerically using a three-dimensional panel method.

Two basic mechanisms of inlet vortex generation were identified [2]. The first of these, which has been alluded to qualitatively by other investigators, is the amplification of ambient (i.e., far upstream) vorticity as the vortex lines are stretched and drawn into the inlet. Quantitative calculations have been carried out to illustrate the central features connected with this amplification, and it was shown that it is the vertical component of ambient vorticity that is by far the more important in this

process.

In contrast to what had been supposed, however, there is another mechanism of inlet vortex formation which had not been recognized previously and which does not require the presence of ambient vorticity. This means that an inlet vortex can, in fact, arise in an upstream irrotational flow, for an inlet in crosswind. In this situation, the vortex is accompanied by a variation in circulation along the length of the inlet, and hence a trailing vortex.

For a given inlet, an important parameter in determining the appearance of an inlet vortex is the capture ratio\*. In the first mechanism, this ratio is important in the determination of the stretching incurred by a vertical vortex line and hence the vorticity amplification. In the second mechanism, this ratio has a strong effect on the separation points on the inlet; consequently, it controls the circulation distribution along the inlet. The effect on flow regimes is shown in Fig. 1 where, at high values of capture ratio, we see the inlet vortex/trailing vortex configuration, whereas at low values, there are two counter-rotating vortices trailing from the rear of the inlet.

The initial investigations, although very revealing of mechanisms, provided only qualitative information on the phenomenon. In order to understand the vortex formation in a more quantitative manner, as well as to answer the second question, a facility was designed and constructed for carrying out quantitative experiments in the MIT Wright Brothers Wind Tunnel [3,4]. The results of this set of experiments are [4,5,6]:

1. Detailed measurements and flow visualization have been carried out for

---

\*Capture ratio is defined as  $U_1 D_1^2 / U_\infty D^2$ , where  $U_1$  is the inlet face average velocity,  $U_\infty$  is the far upstream velocity, and  $D_1$  and  $D$  are the inlet inner and outer diameters respectively.



an inlet operating near a groundplane, in order to obtain quantitative information on the structure of the three-dimensional flow field associated with an inlet vortex.

2. Height to diameter ratio  $H/D$ , and capture ratio  $CR (U_1 D_1^2 / U_\infty D^2)$  were varied over a wide enough range so that the flow regimes encountered ranged from those in which a strong inlet vortex and a single trailing vortex were present, to those in which no inlet vortex existed, but two counterrotating vortices trailed from the inlet.

3. At conditions where a strong vortex was present, measurements were made of the circulation around the inlet and the trailing vortices. It was found that their circulations were approximately equal and opposite (as had been previously hypothesized).

4. Velocity measurements and flow visualization showed that there was a second region of substantial axial vorticity inside the inlet, in addition to that associated with the inlet vortex. This was located at roughly "two o'clock" looking into the inlet.

5. It appears that the (axial) vortex filaments in this second vortical region are a continuation of the vortex lines associated with the trailing vortex. These vortex lines thread out of the inlet, through the capture surface, and trail downstream.

6. The trailing vortex is seen as being due to two "pieces", the above-mentioned vortex lines that come out of the inlet and the vorticity from the boundary layers on the outside of the inlet. This shed vorticity is associated with the change in circulation (round the inlet) along the inlet length, and its magnitude is such as to be consistent with the sum of the inlet vortex and second vortex circulations.

7. Flow visualization studies were also made of the transition between the

inlet vortex/trailing vortex configuration and that of two trailing counter-rotating vortices. It was found that this transition is not gradual (as a function of CR, say) but occurs abruptly at a critical value of this parameter. In this transition, the lower trailing vortex moves downward to become the inlet vortex.

8. A limited parametric study was carried out to quantitatively define the changes in vortex strength and position as H/D and capture ratio are varied. Increasing H/D has a qualitatively, but not quantitatively, similar effect to decreasing CR.

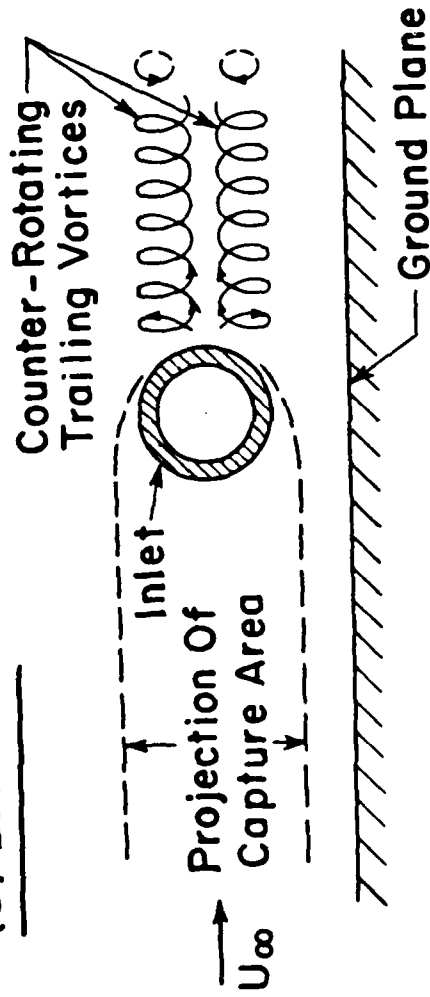
9. Measurements for an inlet operated with an upstream ambient vertical component of vorticity show qualitative agreement with the secondary flow calculations that were performed. It can be seen, however, that there are some nonlinear aspects of the flow (for instance, the mutual induction of the vortices and their images) which this (linearized) calculation does not address.

#### References

1. De Siervi, F., "A Flow Visualization Study of the Inlet Vortex Phenomenon," MIT GTL Report No. 159, 1981.
2. De Siervi, F., et al., "Mechanisms of Inlet Vortex Formation," Journal of Fluid Mechanics, Vol. 124, 1982, pp. 173-207.
3. Liu, W., "Design and Analysis of an Experimental Facility for Inlet Vortex Investigation," MIT GTL Report No. 166, 1982.
4. Liu, W., Greitzer, E.M., Tan, C.S., "Surface Static Pressures in an Inlet Vortex Flow Field," ASME Paper 84-GT-201.
5. Shin, H.W. and Shippee, C., "Quantitative Investigation of the Inlet Vortex Flow Field," MIT GTL Report No. 179, 1984. (Paper also to be submitted for publication.)
6. Shin, H.W., Cheng, W.K., Greitzer, E.M., Tan, C.S., "Inlet Vortex Formation Due to Intensification of Ambient Vorticity," to be submitted for publication.

# Flow Regimes (Inlet In Cross Wind)

(a) Low CR



(b) High CR

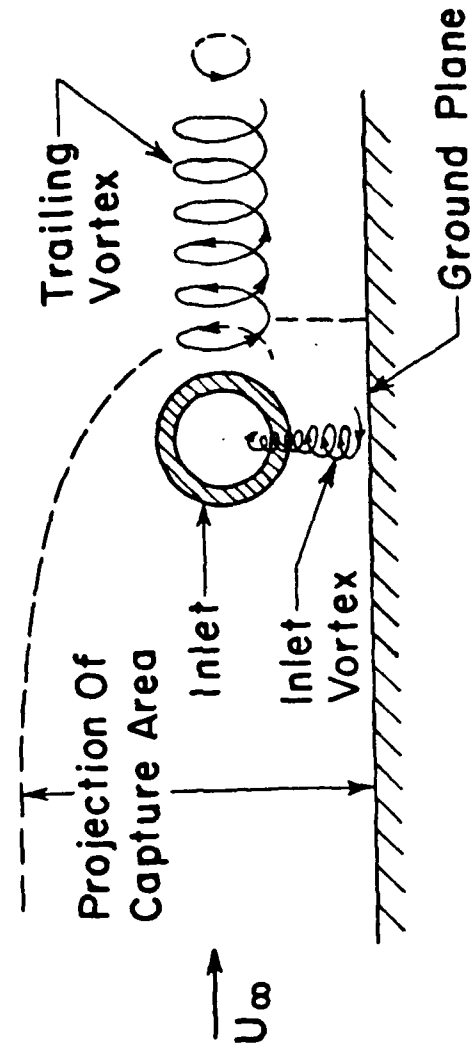


FIGURE 1

TASK IV: INVESTIGATION OF DISCRETE-BLADE AND THREE-DIMENSIONAL FLOWS  
IN HIGHLY LOADED TURBOMACHINES

IVA. 3D BLADE DESIGN IN HIGHLY-LOADED AXIAL COMPRESSORS

The purpose of this project has been to develop a rational method for the design of high deflection blading for axial turbomachines under loading conditions typical of modern machines. Our eventual goal is to provide a method whereby one can determine a blade shape corresponding to a prescribed mean flow field (mean flow turning), as well as the off-design flow field. It could also complement the successful empirically-based techniques used by nearly all engine manufacturers. Emphasis was placed on the inclusion of a variety of three-dimensional effects which are difficult, if not impossible, to model on the basis of cascade data alone. The hope was to enable the designer to extrapolate his own methods with increased confidence to meet the demand for ever higher compressor performance.

Our approach in this study was to emulate, as far as possible, the methods of modern aerodynamics as they are applied to external flows about aircraft. For internal flows, as in turbomachinery, this was made possible by replacing the Biot-Savart "law" of induction\* by the use of the Clebsch transformation technique and then using otherwise classical methods. The advantage of this approach is that the Clebsch variables represent physical quantities such as the blade and wake surfaces, the Bernoulli surface, and the swirl schedule across the blade region in the flow field. In addition, the formulation also takes into consideration the effects of stacking the blade section. Since such a theoretical approach is rather new, as a start, we have made the following assumptions: a) incompressible flow; b) blades in an annulus of constant hub and shroud diameter; and, c) free vortex

---

\*In internal flow, the Biot-Savart law needs images to simulate the presence of internal boundaries and, hence, is extremely complicated.

swirl. These are not inherent restrictions of the theoretical approach but rather are made so as to enable us to explore and clarify the ideas and concepts of the theory before we proceed to relax these assumptions. Since the approach uses the Clebsch representation of inviscid flow, it differs from the conventional time marching (or pseudo-time-marching) technique which uses the primitive Euler equation.

A number of papers have been published by this group which illustrate the progress made under this contract. In Refs. [1] and [2], for example, the design problem for highly-loaded 2D and 3D cascades is addressed at low Mach number and for very thin blades. Here, one is trying to find the appropriate blade camber required to produce a given intra-blade loading distribution. Since the same overall swirl can be produced by a range of swirl schedules, and these in turn correspond to very different pressure distributions, information of this sort provides the designer with some clear choices which can enable him to reduce losses associated with blade boundary layers and/or separation. No linearized approximation is made in the present theory. Successful blade design applications have been made for deflection (up to and including impulse turbines with typical turning angles up to  $120^\circ$ ). Individual blade force coefficients of up to 2.0 were includable. Effort have also been made to obtain the solution iteratively in an efficient manner. The point of including the 2D cascade, as in Ref. [1], was to establish these techniques in as "simple" an environment as possible and to provide a "benchmark" for 3D applications. It also enables us to check our use of the Clebsch approach against the Biot-Savart method. The results of Ref. [2] demonstrate that the three-dimensional calculations can be carried through practically for a variety of realistic compressor geometries and loadings.

In the Master's thesis of T. Dang, it is shown that the same sort of calculation can be carried through with blade thickness (cascade blockage) included, and that blockage effects are quite important in influencing design decisions that may need to be made based on blade pressure distributions. Camber for a given job is very strongly affected by blockage and blockage distribution. Further results of this sort were reported by Dang (Ref. [4]) at a recent ASME conference on computations of internal flows.

As work proceeded along the lines indicated above, it was realized that the fully 3D calculations could become quite cumbersome for more and more realistic applications, largely because of the intricate nature of the blade boundary conditions in shrouded flows. It did not seem to us, however, that full advantage of the periodic nature of the flow had yet been taken. As reported in Ref. [3], these considerations led to a new way of expressing the "singular" nature of the blade-to-blade flow in shrouded cascades, which enormously improved the efficiency of the calculations with little or no sacrifice in accuracy. The resulting method, which we call the "smoothing technique", appears to have wide application for periodic flows, and has been used by us throughout our work in the last two years. It produces results, where applicable, which are in excellent agreement with more classical methods.

Reference [5] and T. Dang's PhD thesis provide the most recent 3D results from the work under this project. Blade design in highly-loaded cascades in the presence of incoming shear has long been recognized as an important and very difficult problem for the designer, because of the necessity of accounting for - and anticipating - the presence of "secondary flow". The induction of altered flow angles by the "secondary" vorticity can vitally alter the blade shape(s) needed to perform a certain task. In

Ref. [5] and more extensively in Dang's PhD thesis - the 3D calculations for this problem are carried through successfully. Illustration is made of the extent and nature of blade shape changes that are required when operation is to occur in a shear-flow environment.

Figure 1 shows the resulting 3D blade profile obtained from this design method for the prescribed job indicated. Note the required spanwise twisting of the blade at the trailing edge due to the presence of secondary flow (see Fig. 3a also). Figure 2 shows the resulting pressure distributions on the blade pressure and suction surfaces at three arbitrary spanwise locations. This blade has parabolic loading characteristics as prescribed.

Figures 3a, 3b and 3c illustrate the Bernoulli surfaces (or total pressure contour) at three different axial locations. Figure 3a clearly shows the spanwise twisting of the blade at the trailing edge, as mentioned earlier.

Figures 4a, 4b and 4c indicate the secondary flow patterns at the corresponding axial locations. The magnitude of the secondary flow velocity is around 10% of the mean inlet velocity. These figures also demonstrate vividly the non-linearity of the flow, including distortions of the Bernoulli and wake surfaces as a function of axial location.

#### Publications

1. Hawthorne, W.R., Wang, C., Tan, C.S., and McCune, J.E., "Theory of Blade Design for Large Deflections: Part I - Two-Dimensional Cascade," Journal for Gas Turbines & Power (ASME Transactions), Vol. 106, No. 2, 1984, pp. 346-354.
2. Tan, C.S., Hawthorne, W.R., McCune, J.E., and Wang, C., "Theory of Blade Design for Large Deflections: Part II - Annular Cascades," Journal for Gas Turbines & Power (ASME Transactions), Vol. 106, No. 2, 1984, pp. 355-365.

3. McCune, J.E., and Dang, T., "Periodic Internal Flows," Proceedings, ASME Conference "Computations of Internal Flows: Methods and Applications," P.M. Sockol and K.N. Ghia, eds., Lib. of Congress Cat. Card No. 83-73578, 1984, pp. 123-128.
4. Dang, T., and McCune, J.E., "Design Method for Highly-Loaded Blades with Blockage in Cascade," Proceedings, ASME Conference "Computation of Internal Flows: Methods and Applications," P.M. Sockol and K.N. Ghia, eds., Lib. of Congress Cat. Card No. 83-73578, 1984, pp. 129-136.
5. Dang, T., and McCune, J.E., "A Three-Dimensional Blade Design Method in Rotational Flow," Proceedings, Int'l Conference on "Inverse Design Concepts in Engineering Sciences" (ICIDES), G.S. Dulikravich, ed., University of Texas, 1984.



# Example

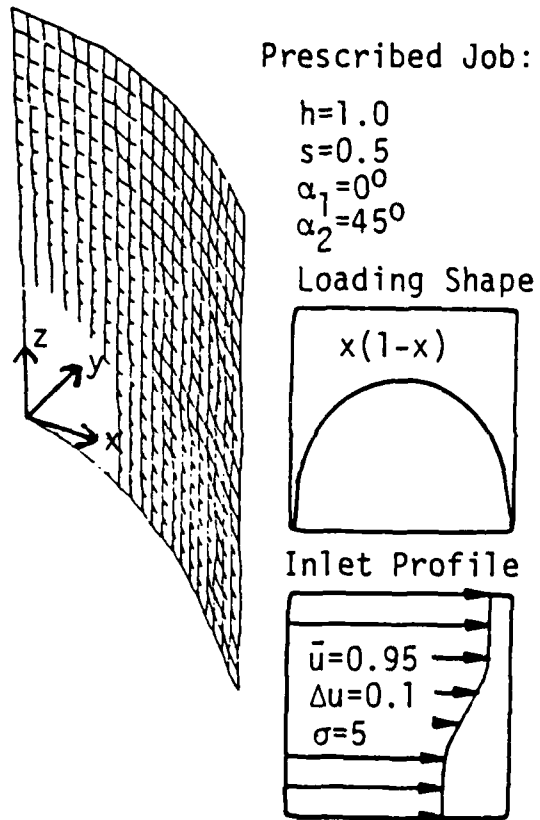


Fig.1: 3D Blade Profile

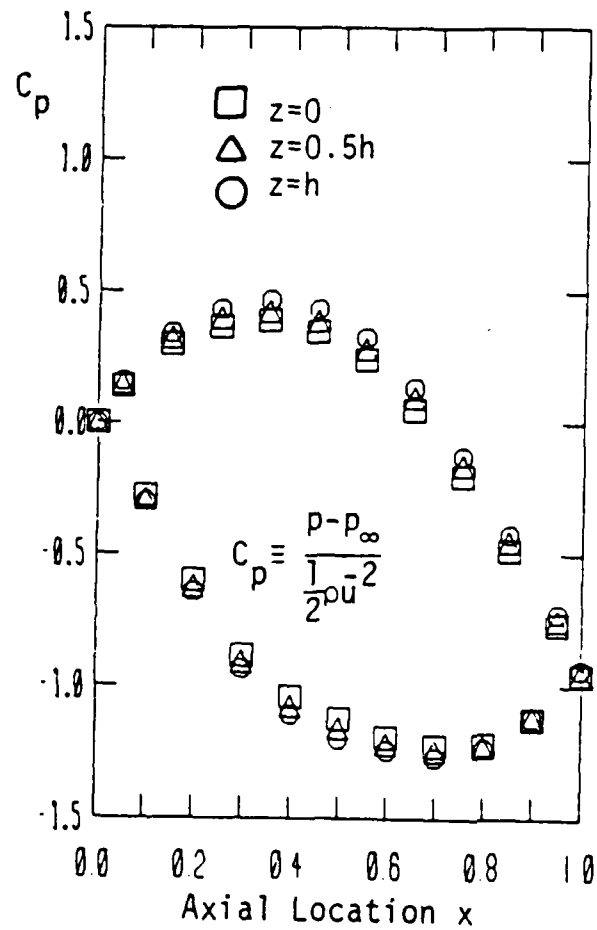


Fig.2: Blade Pressure Distribution

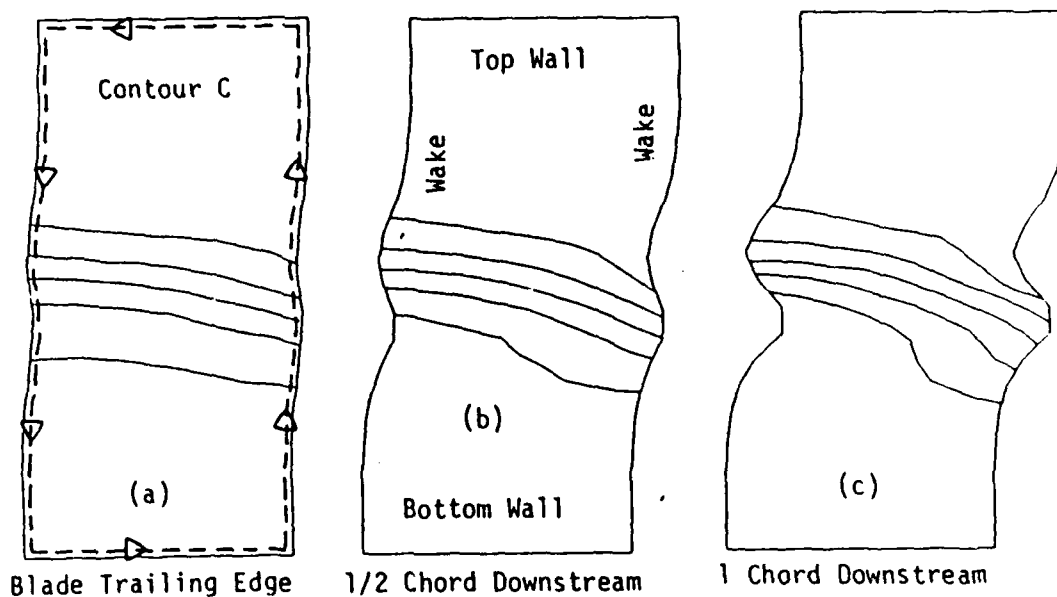


Fig.3: Bernoulli Surfaces at Constant Axial Location (looking upstream)

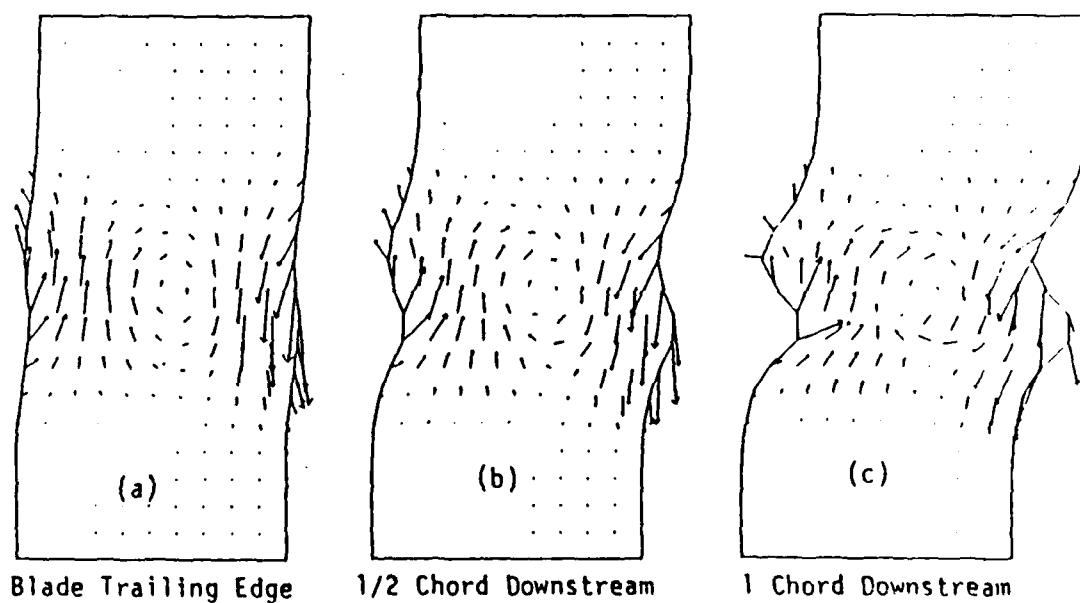


Fig.4: Secondary Flow Pattern at Constant Axial Location

## IVB. NUMERICAL STUDY OF SECONDARY FLOW IN A BEND USING SPECTRAL METHODS

1) Work Accomplished:

A computer code was designed and built to numerically simulate the three-dimensional viscous flow in a bend of rectangular cross-section. This was achieved via the direct solution of an incompressible Navier-Stokes equation using spectral methods based on expansion in Chebyshev Polynomials. A summary of the numerical algorithm is presented in Charts I and II. As reported in our previous progress reports, we used the fractional time-stepping technique to advance the Navier-Stokes equation forward in time in three steps: (1) the nonlinear convective step using the semi-implicit Crank-Nicholson-Adams-Bashforth scheme, (2) the pressure correction step that imposes the incompressibility condition and the inviscid boundary conditions through the solution of Poisson's equation for an intermediate total pressure field, and finally (3) the viscous correction step that imposes the viscous boundary conditions and requires the solution of three Helmholtz equations.

To implement such a solution of Navier-Stokes equations, we developed the following:

- (a) Efficient techniques and software to evaluate and invert Chebyshev series using fast Fourier transform algorithms for Fourier series; this includes single, double and triple Chebyshev series.
- (b) Efficient algorithms for evaluating the derivatives of functions represented by Chebyshev series.
- (c) Three-dimensional Poisson Solver and Helmholtz Solver in cylindrical

co-ordinates (hence Cartesian co-ordinates) using triple Chebyshev series, double Chebyshev series with Fourier series, or second order finite difference approximation in the azimuthal direction.

(d) To achieve task (c), we developed factorization and diagonalization techniques for the Poisson and Helmholtz operators over the Chebyshev collocation points.

(e) Efficient spectral iteration technique for solution of PDE with variable coefficients.

Double precision versions of (a) to (d) are used to establish the convergence, the accuracy, and the reliability of the solution algorithms. (The results of this work will appear in The Journal of Computational Physics.)

In the next section, we present some preliminary results from the computer code.

## 2) Some Preliminary Results

We have run the code for the case of a  $90^\circ$  bend with a square cross-section with Reynolds numbers of 250 and 1000 (with the corresponding Dean's numbers of 289 and 1155 respectively, with the Dean's number defined as  $2(H/R_m)^{1/2} Re$ , where  $H$  is half the width of the cross-section and  $R_m$  is the mean radius of the bend). The inflow velocity is assumed to be of the form  $(1 - 1/\eta^2 (r-\xi)^2) (1-z^2)$ ; simple radial equilibrium is assumed at the inflow plane, which is taken to be at section II in Fig. 1. The cross-stream velocities are assumed to be zero there. The outflow plane is assumed to be at section III in Fig. 1. For the case of  $Re = 250$ , the

initial velocity field is taken to be

$$v_r(t=0) = \frac{0.1\eta}{r\pi} g(\theta) \sin \pi z \left(1 + \cos \frac{\pi(r-\xi)}{\eta}\right)$$

$$v_\theta(t=0) = 0.1h(\theta) \sin \pi z \sin \frac{\pi(r-\xi)}{\eta} (1+r) + \left(1 - \frac{[r-\xi]^2}{\eta^2}\right) (1-z^2)$$

$$v_z(t=0) = \frac{0.1}{\pi} g(\theta) \sin \frac{\pi(r-\xi)}{\eta} (1 + \cos \pi z)$$

where

$$\eta = \frac{1}{2} (r_o - r_i)$$

$$\xi = \frac{1}{2} (r_o - r_i)$$

$$g(\theta) = \theta_o \left\{ \frac{1}{3} \left(\frac{\theta}{\theta_o}\right)^3 - \left(\frac{\theta}{\theta_o}\right)^2 + \left(\frac{\theta}{\theta_o}\right) - \frac{1}{3} \right\}$$

$$h(\theta) = \theta_o^2 \left\{ \frac{1}{12} \left(\frac{\theta}{\theta_o}\right)^4 - \frac{1}{3} \left(\frac{\theta}{\theta_o}\right)^3 + \frac{1}{2} \left(\frac{\theta}{\theta_o}\right)^2 - \frac{1}{3} \left(\frac{\theta}{\theta_o}\right) \right\}$$

in the above,  $r_o$  is the outer radius of the bend

$r_i$  is the inner radius of the bend

$\theta_o$  is the bend angle.

However, in the case where  $Re = 1000$ , the following initial velocity field is used:

$$v_r(t=0) = 0$$

$$v_\theta(t=0) = \left(1 - \frac{[r-\xi]^2}{\eta^2}\right) (1 - z^2)$$

$$v_z(t=0) = 0$$

The results shown in Figs. 2 to 7 are for the case where  $Re = 1000$  after 360 time steps (each time step size is 0.01). (At this time step, the physical variables do not change in the third significant digit.) However, Figs. 9 to 10 show the results for  $Re = 250$  after 835 time steps (at this time step, the physical variables do not change in the fourth significant digit).

In flow through a bend, the fluid is subjected to a centrifugal "force" field which acts more strongly on the faster fluid near the center than the fluid elsewhere. Thus, swirling motion (i.e., the secondary flow) forms at the section normal to the main flow away from the inlet plane. An alternative view is provided by the tilting of the transverse vortex filaments at the inlet plane by the main flow so that these vortex filaments cease to be purely transversed at the latter cross-sectional planes; at these latter cross-sectional planes, there exists vorticity oriented in the main streaming direction known as secondary vorticity, and the associated flow that has to be superimposed on the main stream is called the secondary flow. This phenomenon is highly non-linear, so simple superimposition is not accurate except when the secondary flow effects are weak.

The growth of the streamwise vorticity component, as flow proceeds from the inlet plane to the outlet plane, is shown in Figs. 2a to 2f.

Observe the occurrence of intense streamwise vorticity layers close to the solid walls, and the saturation in the growth of the streamwise vorticity from sectional plane at  $\theta = 69^\circ$  to the outlet plane.

The evolution of the secondary flow pattern from the inlet plane to the outlet plane is shown in Figs. 3a to 3j; as expected, two counter-rotating vortices, one on the upper half plane and one on the lower half plane, slowly evolve and then intensify in strength. Note also the exact symmetry about the mid-height of the section. A quantitative scenario of the streamwise evolution of the velocity profile for each of the velocity components may be seen in Figs. 4 to 6. A radial velocity profile on the  $r-\theta$  plane is shown in Figs. 4a to 4c, and on the  $z-\theta$  plane in Figs. 4d to 4f. Note the slight decrease in the magnitude of the velocity in the neighborhood of the mid-height plane. The corresponding profile for the throughflow velocity is shown in Figs. 5a and 5b on the  $r-\theta$  plane and in Figs. 5c to 5e on the  $z-\theta$  plane; note the shift in the point of maximum throughflow velocity toward the outer region of the bend in Fig. 5b. This is expected since the centrifugal force acts normal to the main direction of the flow so that the throughflow velocity profile is distorted in such a way that its peak is shifted to the outside. Figures 6a to 6c show the axial velocity profile on the  $r-\theta$  plane and Figs. 6d and 6e the profile on the  $z-\theta$  plane. Note the anti-symmetry of the velocity profile, as one would expect from Fig. 3. It is seen from Figs. 4 and 6 that the secondary flow grows more rapidly in the initial section of the bend and very gradually at the later section. In Fig. 7, we show some typical contours of the total pressure field on a few cross-sectional planes to illustrate

the extent of the distortion in the Bernoulli surfaces due to the occurrence of secondary flow.

Finally, for comparative purposes, the corresponding results for  $Re = 250$  are shown in Figs. 8 to 10. Note that the secondary flow seems to be stronger in the case of  $Re = 1000$ , although it should be emphasized that in these preliminary numerical results we have not yet carried out the necessary interpretation in terms of the basic fluid mechanics - this, however, is our eventual objective.

#### Publication

Tan, C.S., "Accurate Solution of Three-Dimensional Poisson's Equation in Cylindrical Co-ordinate by Expansion in Chebyshev Polynomials," accepted for publication in the Journal of Computations



## CHART 1

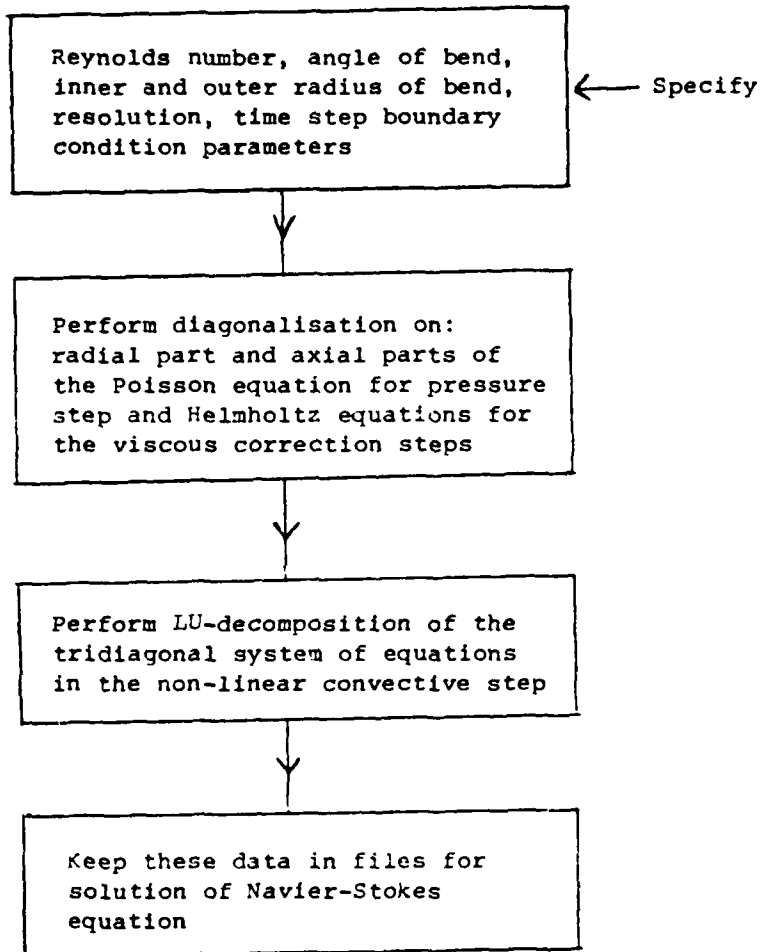
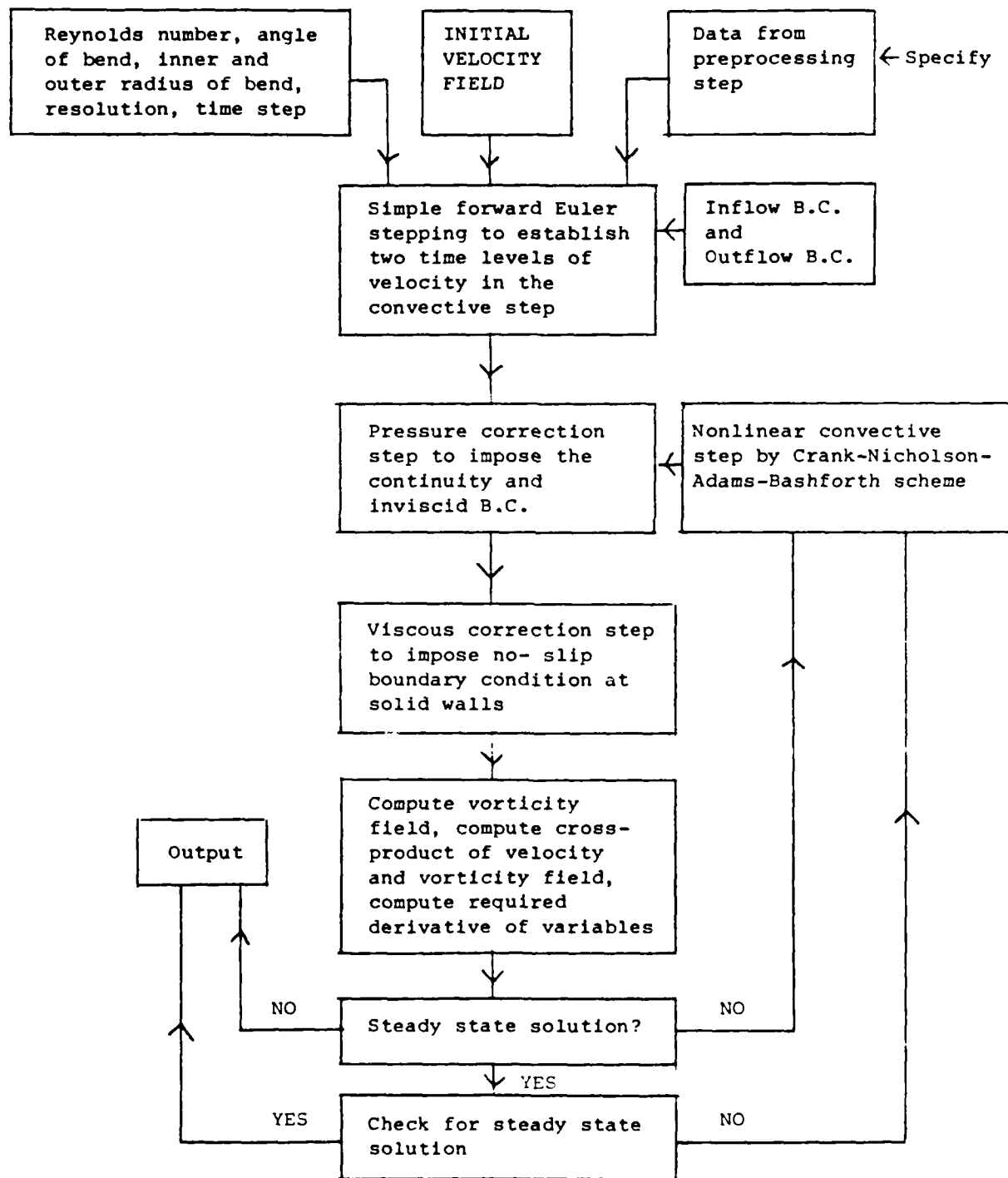
Flow Chart of Numerical Algorithm in Preprocessing Stage

CHART 2

Flow Chart of Numerical Algorithm

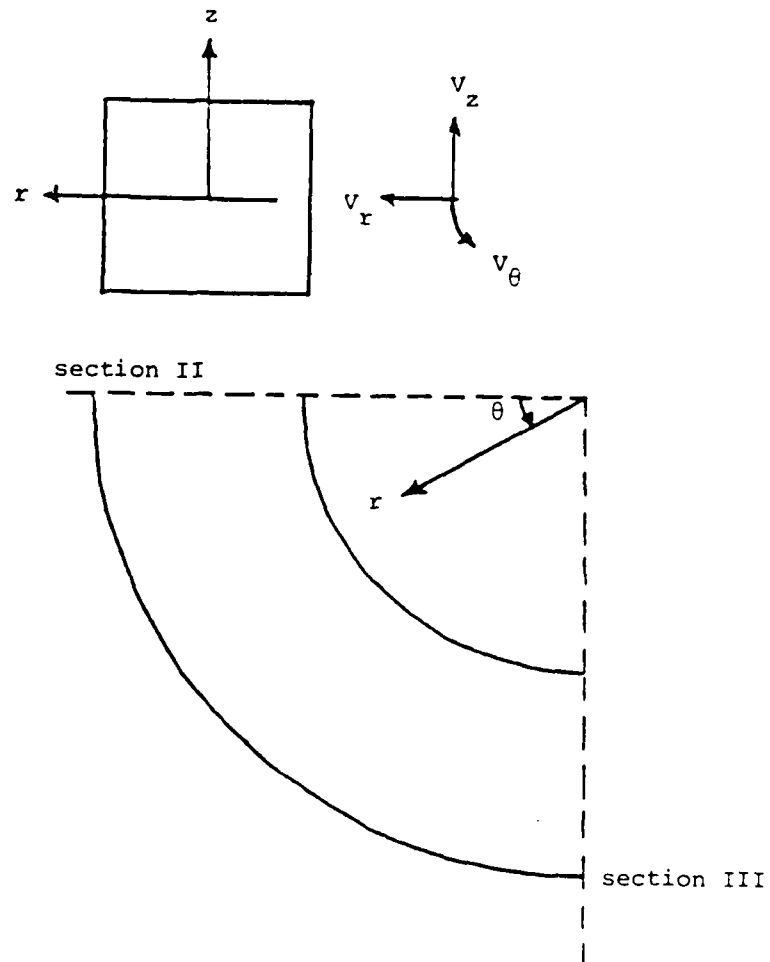
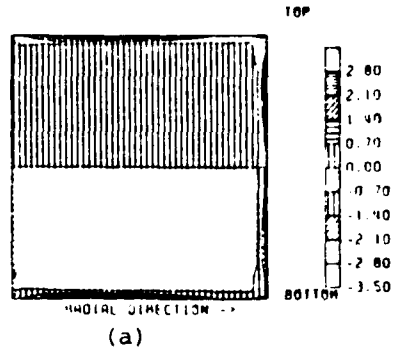
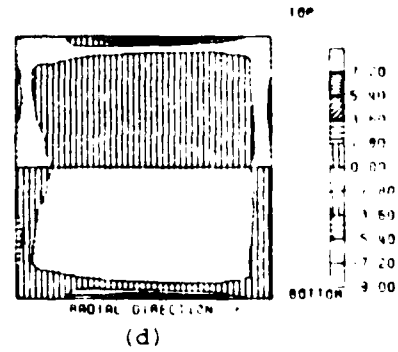


Figure 1: Flow in a bend

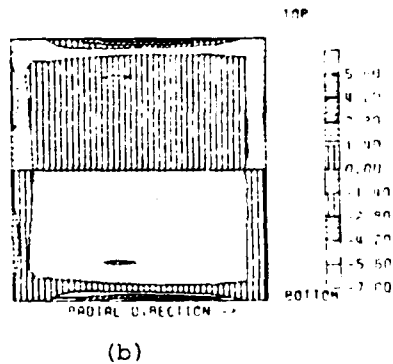
STREAMWISE VORTICITY CONTOUR AT  
 $\theta = 2.308$ ,  $t = 360$ .



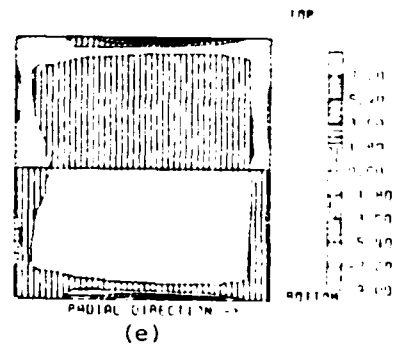
STREAMWISE VORTICITY CONTOUR AT  
 $\theta = 69.230$ ,  $t = 360$ .



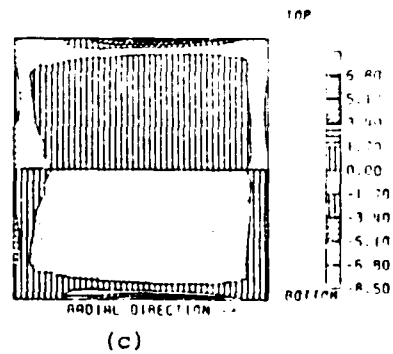
STREAMWISE VORTICITY CONTOUR AT  
 $\theta = 27.692$ ,  $t = 360$ .



STREAMWISE VORTICITY CONTOUR AT  
 $\theta = 83.077$ ,  $t = 360$ .



STREAMWISE VORTICITY CONTOUR AT  
 $\theta = 55.385$ ,  $t = 360$ .



STREAMWISE VORTICITY CONTOUR AT  
 $\theta = 90.000$ ,  $t = 360$ .

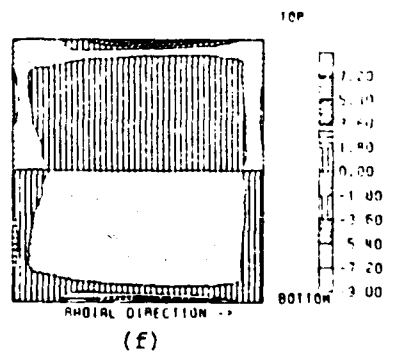


Figure 2: Contour of streamwise vorticity on various cross-sectional planes showing its development in flow through the bend ( $Re = 1000$ )

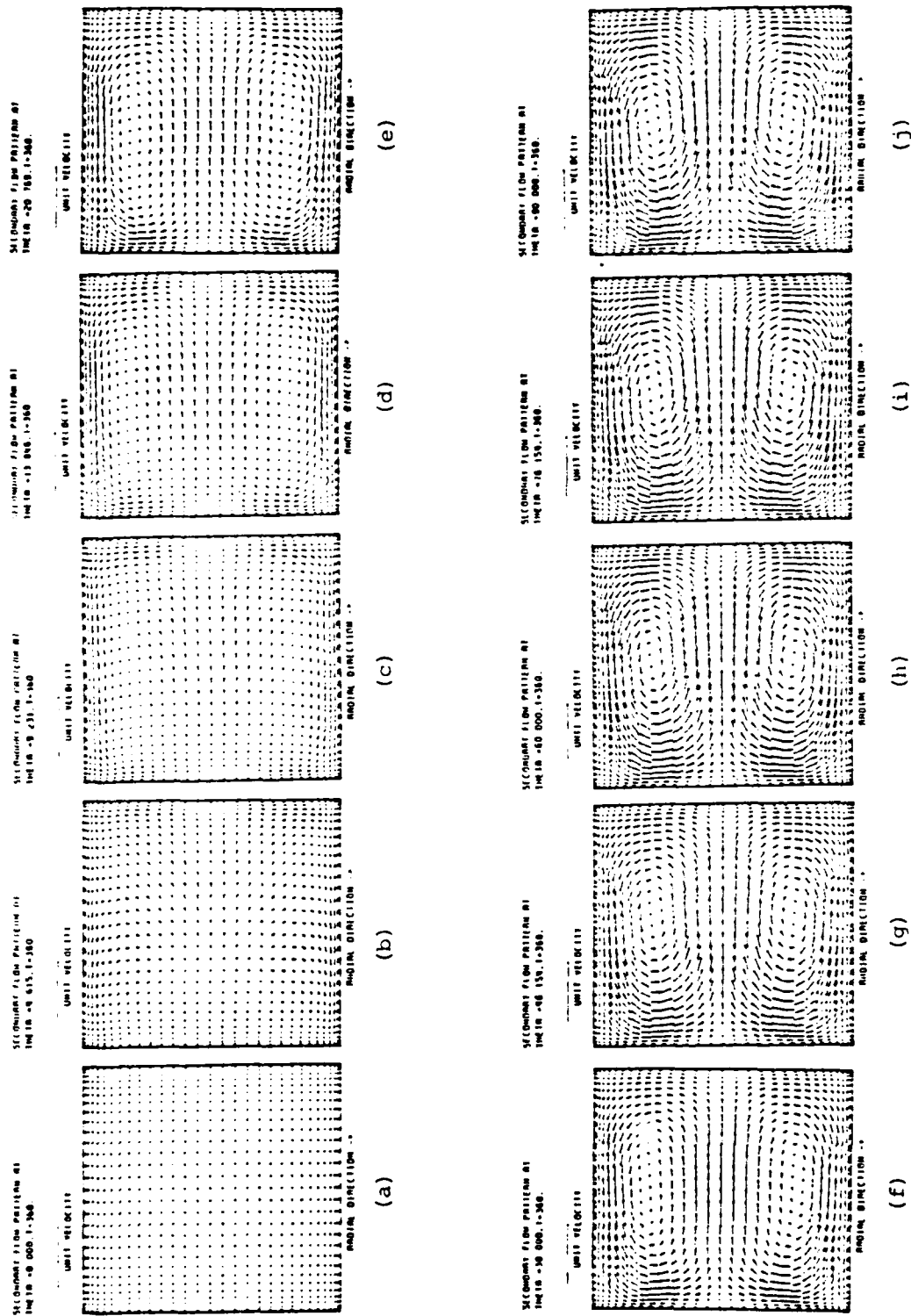
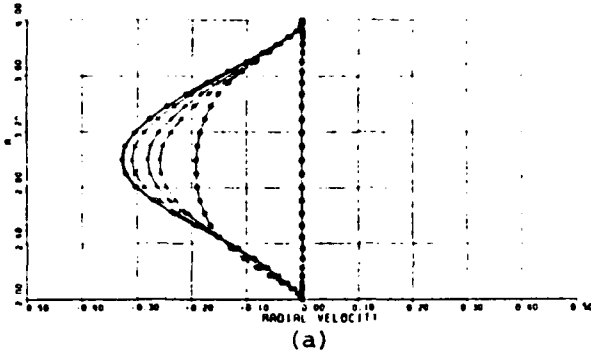
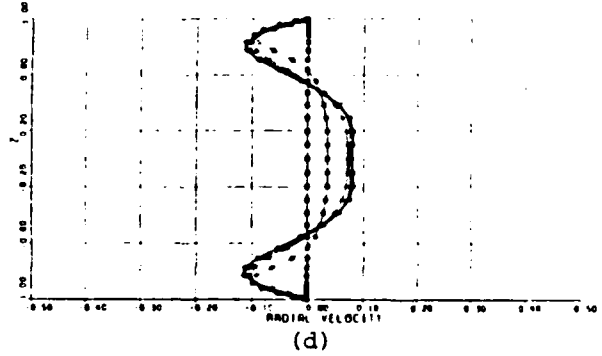


Figure 3: Evolution of secondary flow from inlet plane to the exit plane ( $Re = 1000$ )

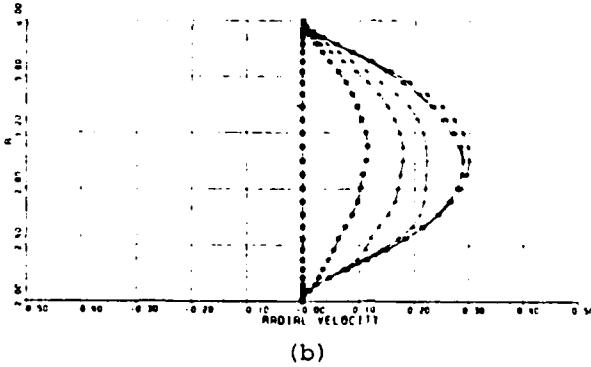
RADIAL VELOCITY VS R  
Z-LOCATION=0.924, TIME=360.



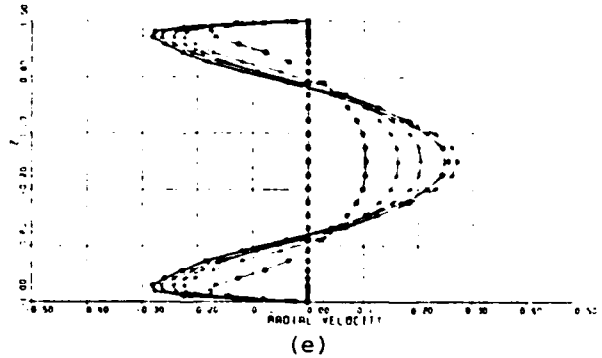
RADIAL VELOCITY VS Z  
R-LOCATION=2.227, TIME=360.



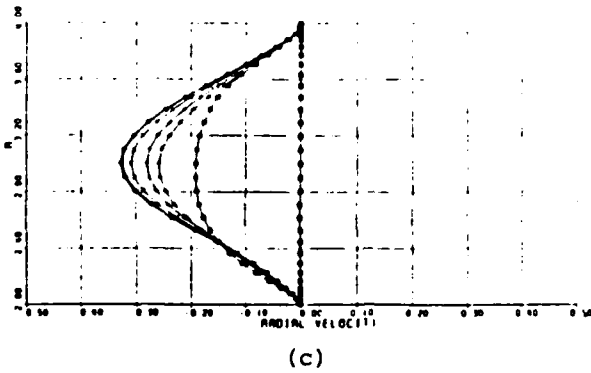
RADIAL VELOCITY VS R  
Z-LOCATION=0.000, TIME=360.



RADIAL VELOCITY VS Z  
R-LOCATION=3.290, TIME=360.



RADIAL VELOCITY VS R  
Z-LOCATION=-0.924, TIME=360.



RADIAL VELOCITY VS Z  
R-LOCATION=5.773, TIME=360.

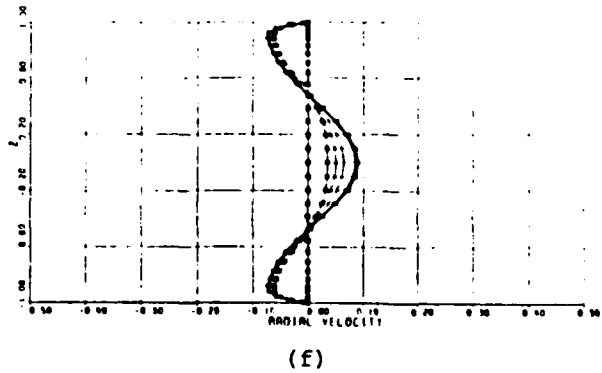
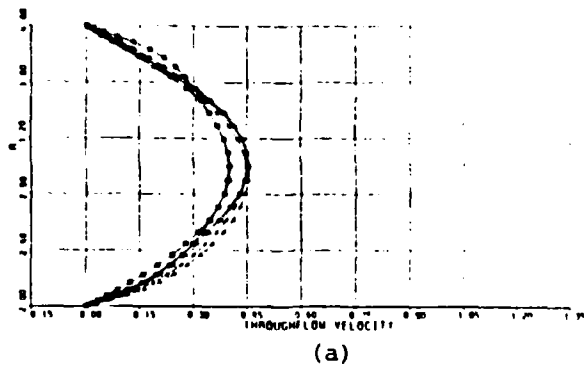
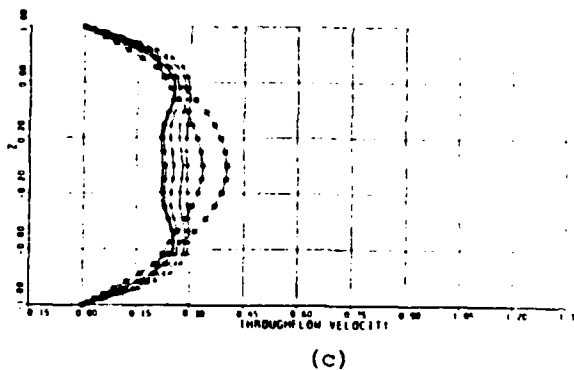


Figure 4: Evolution of radial velocity profiles in the streamwise direction -  
vs R in (a) to (c), and  
vs Z in (d) to (f)

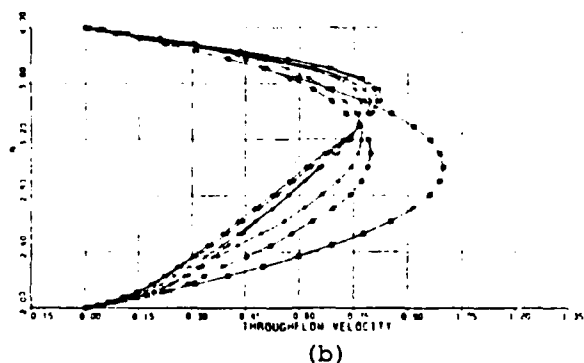
THROUGHFLOW VELOCITY VS R  
Z-LOCATION=0.773, TIME=360.



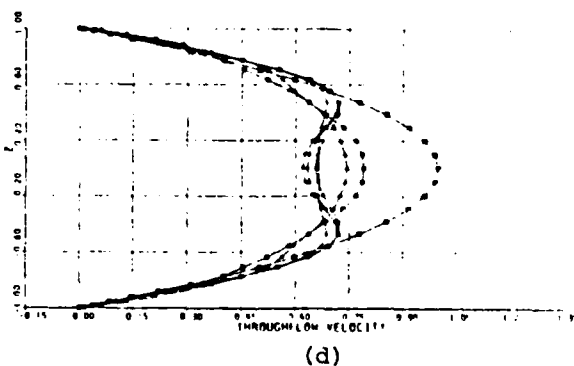
THROUGHFLOW VELOCITY VS Z  
R-LOCATION=2.227, TIME=360.



THROUGHFLOW VELOCITY VS R  
Z-LOCATION=0.000, TIME=360.



THROUGHFLOW VELOCITY VS Z  
R-LOCATION=3.000, TIME=360.



THROUGHFLOW VELOCITY VS Z  
R-LOCATION=3.773, TIME=360.

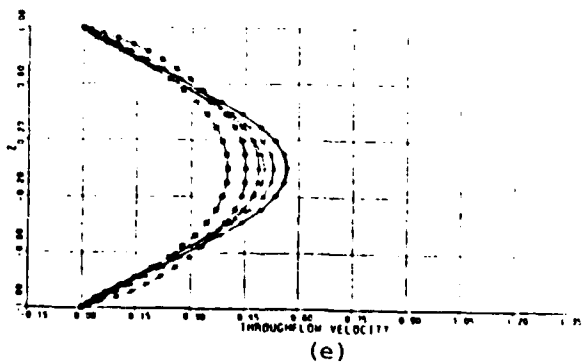


Figure 5: Evolution of throughflow velocity profiles in the streamwise direction ( $Re = 1000$ ) -  
vs R in (a) to (b), and  
vs Z in (c) to (e)

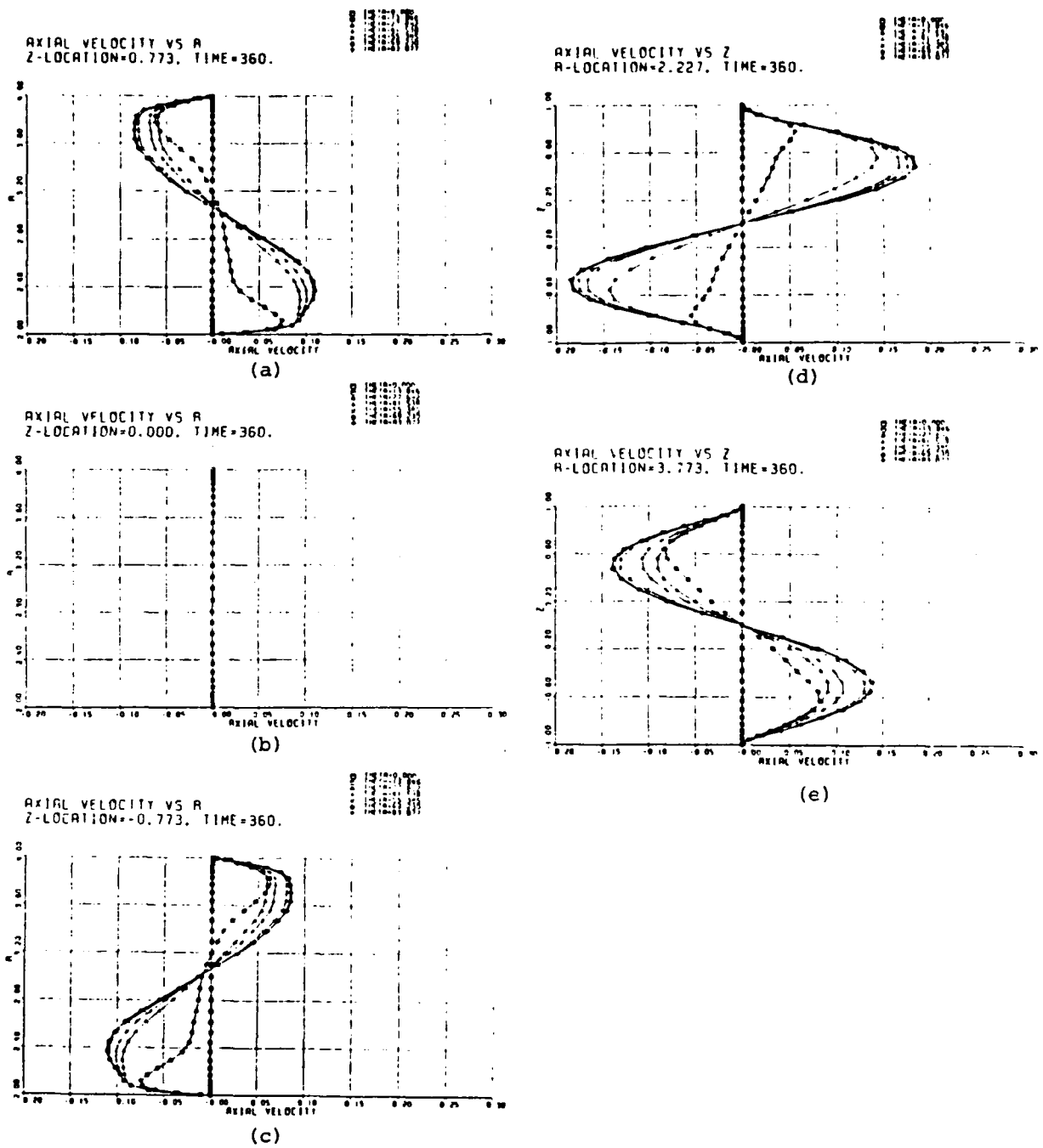
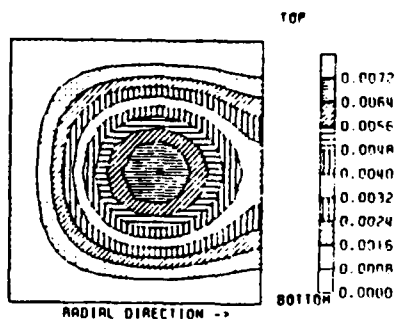


Figure 6: Evolution of axial velocity profiles in the streamwise direction ( $Re = 1000$ ) -  
vs R in (a) to (c), and  
vs Z in (d) to (e)

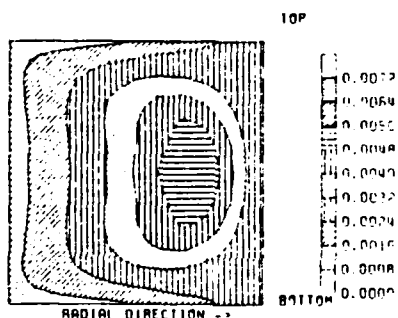


TOTAL PRESSURE CONTOUR AT  
 $\theta = 0.000$ ,  $T = 360$ .



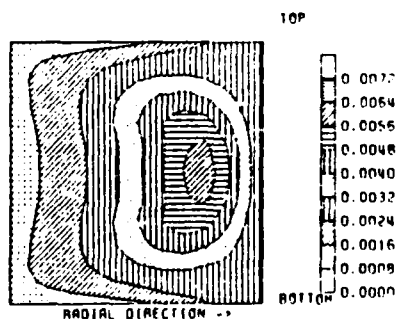
(a)

TOTAL PRESSURE CONTOUR AT  
 $\theta = 41.538$ ,  $T = 360$ .



(b)

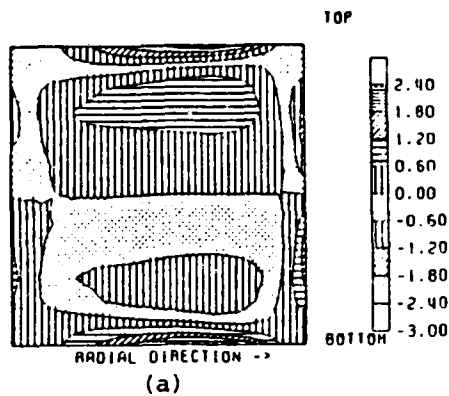
TOTAL PRESSURE CONTOUR AT  
 $\theta = 87.692$ ,  $T = 360$ .



(c)

Figure 7: Stagnation pressure contours on the cross-sectional planes of the bend showing the distortion caused by the resulting secondary flow ( $Re = 1000$ )

STREAMWISE VORTICITY CONTOUR AT  
 $\Theta = 41.538, t = 0.35$ .



STREAMWISE VORTICITY CONTOUR AT  
 $\Theta = 83.077, t = 0.35$ .

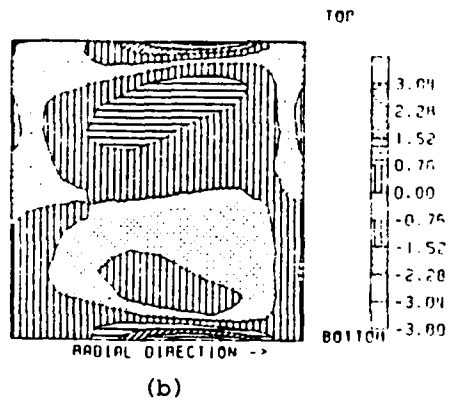
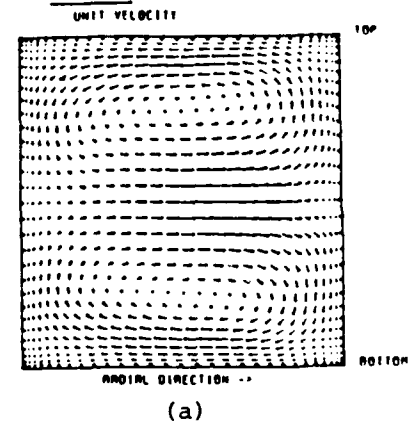
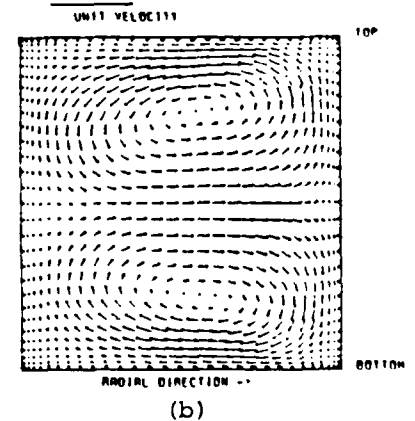


Figure 8: Contour of streamwise vorticity  
 on two cross-sectional planes  
 for the case of  $Re = 250$

SECONDARY FLOW PATTERN AT  
 $\Theta = 30.000, t = 0.35$ .



SECONDARY FLOW PATTERN AT  
 $\Theta = 60.000, t = 0.35$ .



SECONDARY FLOW PATTERN AT  
 $\Theta = 90.000, t = 0.35$ .

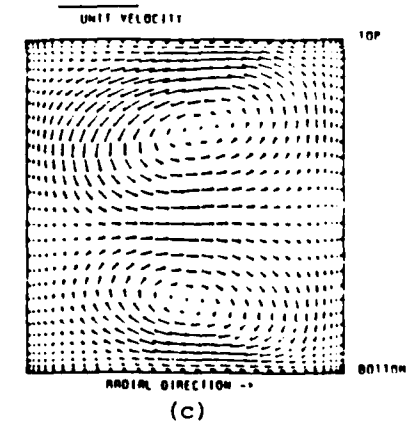


Figure 9: Secondary flow vectors on  
 three cross-sectional planes  
 of the bend for the case  
 where  $Re = 250$

RADIAL VELOCITY VS Z  
R-LOCATION=3.290. TIME=835.

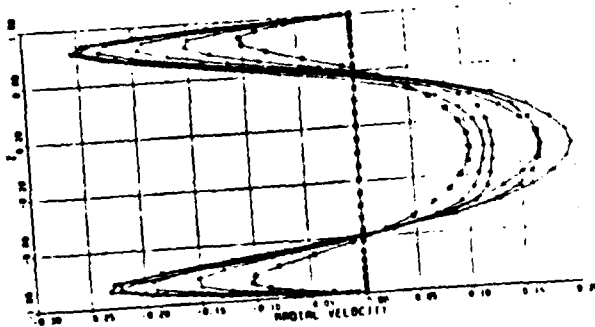


Figure 10a: Evolution of radial velocity profile vs Z in the streamwise direction for the case where  $Re=250$

TANGENTIAL VELOCITY VS R  
Z-LOCATION=0.773. TIME=835.

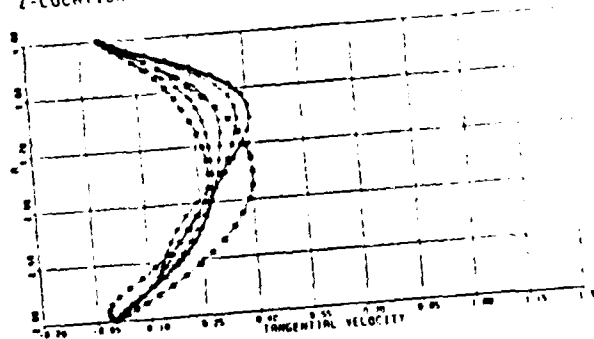


Figure 10b: Evolution of throughflow velocity profile vs R in the streamwise direction for the case where  $Re=250$

AXIAL VELOCITY VS Z  
R-LOCATION=3.773. TIME=835.

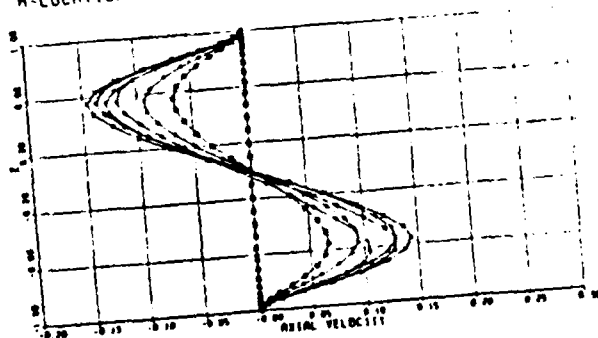


Figure 10c: Evolution of axial velocity profile vs Z in the streamwise direction for the case where  $Re=250$

## IVC. NON-AXISYMMETRIC COMPRESSIBLE SWIRLING FLOW IN TURBOMACHINE ANNULI

The behavior of non-axisymmetric disturbances in compressible swirling flows, typical of those found in turbomachine annuli, was examined using an analysis based on the Clebsch transformation of the equations of motion in a reduced flow form. For the flows analyzed, the different types of disturbances (vorticity, entropy, and pressure) were shown to interact strongly in the presence of swirl. Numerical examples presented show that mean swirl level and mean Mach number can have a strong influence on the downstream evolution of the nonaxisymmetric disturbances. In particular, at high subsonic Mach number in regions of high swirl, the amplitude of the non-axisymmetric disturbances can show oscillations with decreasing amplitude, as a function of downstream distance. A simple flow model was also used to examine the static pressure nonuniformities that can occur in one class of these non-axisymmetric flows. The qualitative behavior described by this (much) simpler model was also deduced from the general analysis.

References

1. Tan, C.S. and Greitzer, E.M., "Non-Axisymmetric Compressible Swirling Flow in Turbomachine Annuli," to be published in AIAA Journal.
2. Tan, C.S. and Greitzer, E.M., "Non-Axisymmetric Compressible Flow Through Annular Actuator Disks," MIT GTL Report No. 169, October 1982.

3. PROGRAM PERSONNEL (10/81 - 10/84)

Principal Investigators:

Edward M. Greitzer  
Professor of Aeronautics and Astronautics  
Director, Gas Turbine Laboratory

Jack L. Kerrebrock  
R.C. Maclaurin Professor  
and Department Head  
Aeronautics and Astronautics

William T. Thompkins, Jr.  
Associate Professor of Aeronautics and Astronautics

James E. McCune  
Professor of Aeronautics and Astronautics

Co-Investigators:

Alan H. Epstein  
Associate Professor of Aeronautics and Astronautics  
Associate Director, Gas Turbine Laboratory

Choon S. Tan  
Research Associate

Collaborating Investigators:

Eugene E. Covert  
Professor of Aeronautics and Astronautics  
Director, Center for Aerodynamic Studies

Sir William R. Hawthorne  
Senior Lecturer

Wai K. Cheng  
Soderberg Assistant Professor of Mechanical Engineering

Hyoun-Woo Shin  
Post-Doctoral Associate

Robert Haines  
Research Associate

## Graduate Research Assistants:

9/80 - 8/82	Peter Cheng*
9/81 - 11/82	Philippe Kletzkine*
9/80 - 8/82	Wen Liu*
9/80 - 12/83	Wing-Fai Ng**
9/83 - Present	Mark Johnson (AFRAPT Student)
9/81 - Present	Thong Dang*
9/83 - 3/84	Petros Kotidis
9/82 - 3/84	Cheryl Shippee*
9/82 - 12/83	Gilles Thevenet*
9/79 - 6/84	Siu Shing Tong**
9/84 - Present	Norman Lee
9/83 - Present	Mark Drela

\* S.M. Degree Completed

\*\*Ph.D Thesis Completed

#### 4. INTERACTIONS

As described in previous reports, there are strong interactions between the Gas Turbine Laboratory and the aircraft engine industry, as well as Air Force, NASA and other government laboratories. We have an active seminar program to bring speakers from industry and/or government to MIT. In addition, MIT has had a long-standing commitment to research on gas turbines and we have maintained strong coupling with aircraft engine companies. There is thus a substantial amount of technical interchange on related topics between MIT personnel and those at the aircraft engine companies.

## 5. DISCOVERIES, INVENTIONS AND SCIENTIFIC APPLICATIONS

### Discoveries

We demonstrated (for the first time) that compressor hub treatment can markedly improve the stall margin of an axial compressor stator row.

### Inventions and Scientific Applications

A transonic flow computation procedure, having stagnation pressure errors on the order of 1%, has been developed for turbomachinery cascades.

Also, a total temperature probe for making high frequency response measurements in a transonic compressor stage has been developed.



## 6. SUMMARY AND CONCLUSIONS

It appears that progress has been made on all the tasks listed under the Multi-Investigator Contract. The main items of note are, by task:

- I.A Two inverse (design) methods, applicable to the full Mach number range encountered in high speed axial compressors, have been developed. One method, based on time-marching solutions to the Euler equations, worked well for supersonic flows but was too computationally expensive for practical design work. The second method, which was based on a steady state Euler equation solver for streamtubes, has been applied to several "simple" flows with good success and shows considerable promise for general internal and external flow problems.
- I.B A high frequency response total temperature and pressure probe has been invented which has permitted, for the first time, time-resolved measurements of the local efficiency in high speed turbomachinery. These measurements revealed the presence of high frequency flow oscillations (caused perhaps by rotor shock system instability); these may account for 1% of the stage loss in transonic compressors.
- II. The use of a grooved hub treatment under a stator row has been shown (for the first time, as far as the authors are aware) to result in a substantial increase in blade row stable flow range and peak pressure rise. Detailed measurements indicate the strong role of the bulk mass and momentum transfer between the flow in the grooves and that in the passage endwall region.
- III. A new mechanism of inlet vortex formation has been discovered. First of a kind quantitative measurements of vortex strength and position have been made at conditions representative of aircraft take-off.
- IV.A An analytic design method has been developed to determine 3D blade shapes required to create specified loadings or swirl schedules in internal flows typical of high performance turbomachinery. An improved analytic description of internal periodic flows was discovered which greatly enhances computational efficiency.
- IV.B A formulation and a computer code have been developed for the simulation of three-dimensional viscous flow in a bend using spectral methods. Initial numerical results have been obtained showing the development of the strong streamwise vorticity in the bend.
- IV.C A theory has been developed to analyze the behavior of non-axisymmetric disturbances in a strongly swirling flow, typical of those in a turbomachinery environment. In this situation, the vorticity, entropy, and pressure disturbances are strongly coupled due to the presence of the swirl.

In addition, we have found the vehicle of a multi-investigator program useful. It has given us flexibility in direction, as well as helped ensure the "critical mass" of students and staff that is necessary for any sustained progress on the complex problems that are characteristic of modern turbomachinery fluid mechanics.

**END**

**FILMED**

**3-85**

**DTIC**